

Exploration of Diverse Interactions of L-Methionine in Aqueous Ionic Liquid Solutions: Insights from Experimental and Theoretical Studies

Sukdev Majumder, Anuradha Sinha, Debadrita Roy, Biswajit Ghosh, Narendra Nath Ghosh, Tanusree Ray, Vikas Kumar Dakua, Anupam Datta, Indu Bhusan Sarkar, Subhankar Choudhury, Ashim Roy, Nitish Roy, and Mahendra Nath Roy*



Cite This: *ACS Omega* 2023, 8, 12098–12123



Read Online

ACCESS |



Metrics & More

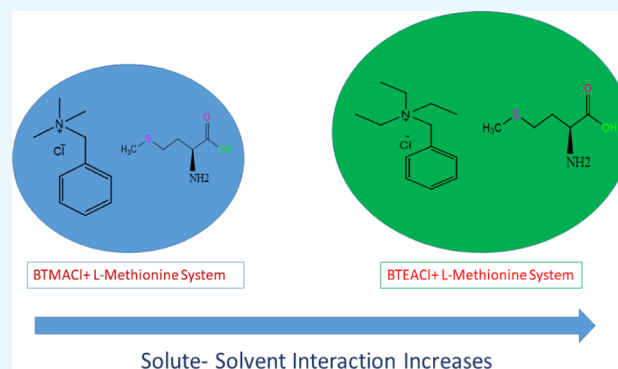


Article Recommendations



Supporting Information

ABSTRACT: Here, we have investigated some physicochemical parameters to understand the molecular interactions by means of density (ρ) measurement, measurement of viscosity (η), refractive index (n_D) measurement, and conductance and surface tension measurements between two significant aqueous ionic liquid solutions: benzyl trimethyl ammonium chloride (BTMAC) and benzyl triethyl ammonium chloride (BTEAC) in an aqueous L-methionine (amino acid) solution. The apparent molar volume (Φ_v), coefficient of viscosity (B), and molar refraction (R_M) have been used to analyze the molecular interaction behavior associated in the solution at various concentrations and various temperatures. With the help of some important equations such as the Masson equation, the Jones–Doles equation, and the Lorentz–Lorenz equation, very significant parameters, namely, limiting apparent molar volumes (Φ_v^0), coefficient of viscosity (B), and limiting molar refraction (R_M^0), respectively, are obtained. These parameters along with specific conductance (κ) and surface tension (σ) are very much helpful to reveal the solute–solvent interactions by varying the concentration of solute molecules and temperature in the solution. Analyses of $\Delta\mu_1^{0\#}$, $\Delta\mu_2^{0\#}$, $T\Delta S_2^{0\#}$, $\Delta H_2^{0\#}$, and thermodynamic data provide us valuable information about the interactions. We note that L-Met in 0.005 molality BTEAC ionic liquid at 308.15 K shows maximum solute–solvent interaction, while L-Met in 0.001 molality BTMAC aqueous solution of ionic liquid at 298.15 K shows the minimum one. Spectroscopic techniques such as Fourier transform infrared (FTIR), $^1\text{H-NMR}$, and UV–vis also provide supportive information about the interactions between the ionic liquid and L-methionine in aqueous medium. Furthermore, adsorption energy, reduced density gradient (RDG), and molecular electrostatic potential (MESP) maps obtained by the application of density functional theory (DFT) have been used to determine the type of interactions, which are concordant with the experimental observations.



1. INTRODUCTION

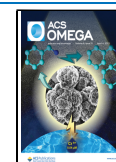
For improvement in the pharmaceutical as well as food industrial fields, use of thermodynamic properties like surface tension and volumetric assets in the case of small-chain amino acids (AAs) in the presence of an aqueous environment is needed, which are vital factors to determine the various fluid-phase transport methods.¹ It is a well-known fact that the different thermodynamic assets of AAs in an aqueous medium of electrolyte offer us the necessary information about proteins in the case of conformational stability in a particular solution. Furthermore, the solubility, denaturation, separation into subunits, enzyme activities, purification, as well as solute–solvent and solute–solute interactions can also be obtained from the different thermodynamic information.^{2–5} In fact, it is very important to know about the thermodynamic properties and thermophysical knowledge of ionic liquids (ILs) to

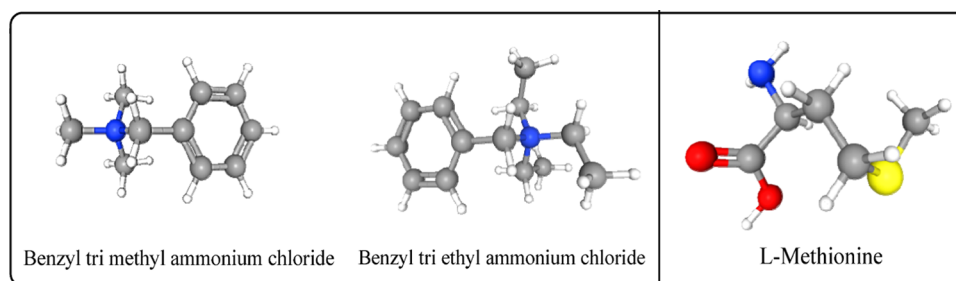
optimize and control the extraction of biomolecules in aqueous media. Knowledge of their thermophysical and thermodynamic properties is required. Using an electrolyte with AAs in an aqueous solution, the interaction behavior can also be obtained from the extensive volumetric and viscometric studies.^{2,6–8} In these connections, we have studied the volumetric assets of amino acid in the presence of an IL solution, which will be a very useful factor for obtaining information about the diverse interactions happening in these solutions, and among them,

Received: December 16, 2022

Accepted: March 8, 2023

Published: March 24, 2023



Scheme 1. Ball-and-Stick Model Three-Dimensional Representation of Benzyl Trimethyl Ammonium Chloride, Benzyl Triethyl Ammonium Chloride, and L-Methionine

hydrophobic and electrostatic interactions are generally the most common.

Studying these types of interactions in the above-described sections provide us with a very important vision about the stability of conformation, as well as the characteristic of the unfolding nature that occurs in the structure of globular proteins.

The valuable data of AAs in aqueous solutions containing salts obtained from different thermodynamic variables help to understand the solute–solute and solute–solvent interactions. Due to the presence of salt, the characteristics of conformational changes in an aqueous medium of AAs are affected; as a result, the denaturation of proteins takes place in a biological process.

Therefore, keeping in mind both the importance and applicability, it is very necessary to investigate the thermodynamic assets of an ionic liquid and amino acid mixture, which provides valuable information regarding the solvation of these biomolecules.⁹ To understand the transport phenomenon of electrolytes it is very important to study the atomistic description of solute solvent interactions. The electrical conductance depends mostly on the variable concentration of the electrolyte and solvent viscosity in a solution medium. Ionic solvation plays a very crucial role in studying the different applications of salt in an aqueous medium.

The physicochemical and thermodynamic properties of amino acids (AAs) are of considerable interest as these biomolecules are the building blocks of all living organisms and are found to provide valuable information that leads to a good conceptual idea about proteins. The direct study of interactions of proteins is not possible due to their large and complex nature. Therefore, one of the suitable approaches is studying the interaction criteria of a model compound of proteins, e.g., amino acids mixing in aqueous solutions. Furthermore, due to the absence of experimental thermodynamic records of proteins, amino acids can serve as useful models in estimating their properties. For the preparation of mixed solvents, water is used as a solvent because it has a unique nature in its structure, and in this case, the hydrophobic force of interaction plays a very important role between water and the protein, providing stability to the protein, and this is very important to stabilize the structure of native globular proteins.¹⁰ The choice of L-methionine, benzyl trimethyl ammonium chloride (BTMAC), and benzyl triethyl ammonium chloride (BTEAC) is made due to the large hydrophobicity property of L-methionine and the ionic liquid. They are based on natural, biorenewable raw materials, and this amino acid has a pharmaceutically and cosmetically acceptable counterion of the chosen ionic liquids.

An ionic liquid, IL,¹¹ is a salt in the liquid state having a low melting point of nearly illogical temperatures such as 373 K. The special nature of ionic liquid makes it unique. The unique nature of ionic liquids is characterized by their small vapor pressure, thermally very stable nature, very high liquidus range, ability to dissolve a variety of chemicals, and very large electrochemical window. There are some inorganic and biocatalytic reactions in which ionic liquids are favorable as designer solvents and green alternatives in place of volatile organic solvents. Ionic liquids are used in the processing of biomass as heat-transfer fluids and in the field of electrochemistry, specially in batteries and solar cells, as electrically conductive liquids. It is very important to apply ionic liquids when making analytical equipment. In lithium-ion batteries, ionic liquid is used as an electrolyte. It is also used as a capacitor and to make metal plating baths.^{12–18}

The various chemicals that are used in this experiment find extensive industrial usage. BTMAC (Scheme 1) is soluble in water and has lyophilic and hydrophilic groups. There are many two-phase organic positional changing processes where BTMAC is used as a catalyst in the case of a phase-transfer process. BTMAC has been applied in the fields of pharmaceuticals, agrochemicals, and polymer industries. In the field of oil industries, BTMAC plays an important role as an erosion inhibitor. In the cases of polycondensation reactions, a lipotropic phase-transfer catalytic agent, benzyl triethyl ammonium chloride (Scheme 1), is used in the phase-transfer catalysis (PTC) process to catalyze the process under biphasic conditions to convert low-molecular-weight polymers to high-molecular-weight polymers. In human bodies, L-methionine (Scheme 1) or L-Met is used as a very essential amino acid. It plays a very critical role in the metabolism process and in curing many diseases. Involvement of L-Met in the production of meat, fish, and dairy is very important. This amino acid is also found in many cell functions. It is used to prevent liver damage in acetaminophen (Tylenol) poisoning. It is also used for increasing urine acidity in kidneys, curing liver disorders, and during wound healing in our bodies. The amino acid methionine can be made from all plants as well as some forms of bacteria. Cobalamin enzyme is used to synthesize some mammalian tissues and many bacteria, whereas all of the plants and some bacteria synthesize it from homocysteine. For determination of psychotic disorder in a patient, different amino acids such as methionine, homocysteine, and cystathionine are used to measure the cerebrospinal fluid levels in the brain.¹⁹

The application of salt in the case of the current technology is well assumed by the study of solvation of ions or association of ions in solution. The way of solvation of ions associated with

Table 1. Detailed Information about the Chemicals^a

chemical name with molecular formula	CAS no.	abbreviation of chemicals	provider	purity/mass fraction	^b purification method	^c analysis method	^{c*} water content (w %)	molar mass/g·mol ⁻¹
benzyl trimethyl ammonium chloride (C ₁₀ H ₁₆ ClN)	56-37-1	BTMAC	Sigma-Aldrich (India)	≥0.99	heat under vacuum desiccator	Karl–Fischer Titrator	0.09%	185.69
benzyl triethyl ammonium chloride (C ₁₃ H ₂₂ ClN)	56-93-9	BTEAC	Sigma-Aldrich (Germany)	≥0.98	heat under vacuum desiccator	Karl–Fischer Titrator	0.15%	227.77
L-methionine (CHNOS)	63-68-3	L-Met	Sigma-Aldrich (Japan)	≥0.99	recrystallization	-	-	149.21

^aNo further purification of used chemicals was performed. ^{c*}The (w %) values of water in two ionic liquids (BTMAC, BTEAC) were determined using the Karl–Fischer titrator and were found to be less than 0.09 and 0.15%, respectively. # Considering the purity of mass of the chemicals, the combined standard uncertainty in molality is expected to be ±0.0147 mol·kg⁻¹. ^bIndicates purification method. ^cIndicates analysis method.

it almost depends on the association nature of the ion of electrolytes and also the type of solvent or mixtures of solvents.^{20–22} The determination of the behavior of ion associations and solvation processes that associate in solution is achieved from conductivity measurements. Besides, the extent of association of ions and the interaction among the solvent totally depend on the viscosity data and relative permittivity of the solvent used in the study of the experiment. For elucidating the different interactions that occur between the amino acid and ionic liquids, various properties such as volumetric, viscometric, refractometric, conductometric, and surface tension are very useful aspects. In this regard, connections, volumetric, viscometric, and thermodynamic variables such as apparent molar volume (Φ_v), limiting apparent molar volume (Φ_v^0), viscosity *B*-coefficients, dB/dT , $\Delta\mu_1^{0\neq}$, $\Delta\mu_2^{0\neq}$, $\Delta S_2^{0\neq}$, and $\Delta H_2^{0\neq}$ have also been studied and elucidated to have a better understanding of such interactions in aqueous ternary (H₂O + IL+ amino acid) systems.

To study the possible interactions associated with the molecule of amino acid (L-methionine) with two ionic liquids (BTMAC and BTEAC), binary mixtures of (AA + IL), which are dissolved in D₂O, have been done by the ¹H-NMR spectroscopy technique. For the interpretation of various molecular interactions associated with the amino acid (AA) and ionic liquids (ILs), Fourier transformation infrared (FTIR)-spectroscopy measurements were carried out. In this measurement, solid KBr is mixed with a binary mixture of amino acid with two ILs.

Our present work deals with one amino acid (L-methionine) and two very significant ionic liquids, namely, BTMAC and BTEAC. We carried out here this investigation to explore diverse molecular interactions incorporated with amino acid and ionic liquids with the help of thermodynamic data and transport phenomenon at three temperatures (298.15, 303.15, and 308.15 K), which are supported by spectroscopic studies.

Furthermore, the mode of interactions was obtained from density functional theory (DFT) based on adsorption energies, which were validated with experimental results.

2. EXPERIMENTAL DETAILS

2.1. Materials. For our experiment, we have used here benzyl trimethyl ammonium chloride (the chemical formula and molecular weight of this ionic liquid are C₁₀H₁₆ClN and 185.69 g·mol⁻¹, respectively), benzyl triethyl ammonium chloride (the chemical formula and molecular weight of this ionic liquid are C₁₃H₂₂ClN and 227.77 g·mol⁻¹, respectively), and L-methionine (the chemical formula and molecular weight

of this amino acid are C₅H₁₁NO₂S and 149.21 g·mol⁻¹, respectively). Here, all of the used chemicals of purist's grade were obtained from Sigma-Aldrich India, Germany and Japan, and they were bought from an acceptance authority. Approximately 0.98, 0.99, and 0.99 fractions of mass purity of the used compounds were taken for our experiment. L-Methionine was used after recrystallization of an ethanol–water mixture. The water contents in both ionic liquids were found to be less than 0.09 and 0.15% upon treatment with Karl–Fischer analysis. The ILs were characterized using ¹H-NMR (Bruker AVANCE DRX 400 NMR spectrometer) to rule out the possibility of any major impurities in samples. The ¹H-NMR spectral data of BTMAC and BTEAC in the D₂O solvent at 298.15 K are reported in the Supplementary Information (Figures S7 and S8). The ionic liquids and amino acids were taken for the experiment without further purification. A vacuum desiccator was used to dry the chemical samples at room temperature for at least 72 h over blue silica gel before use. To prepare the solutions for our experiment accurately, approximately 0.7 μS·cm⁻¹ conductivity with doubly distilled deionized water was used. All of the information on the samples are listed in Table 1.

2.2. Experimental Procedures. The vibrating-tube density meter (model: Anton Paar DMA4500M DMA, Austria) was considered to measure the density (ρ) of the experimental solutions. In the digital (Anton Paar DMA4500M) density meter, the mechanical oscillation of the U-tube, e.g., electromagnetic oscillation, is converted into an alternating voltage of identical frequency. To evaluate the period τ with high resolution and standpoints in simple relation to the density ρ of the sample in the oscillator. The apparatus of the density meter was calibrated by passing deionized, triply distilled water and then dry air.²³ An automatic built-in Peltier device was used to keep the temperature fixed within the range ±0.01 K. The range for overall uncertainty in density measurements was ±0.00089 g·cm⁻³.

The measurement of viscosity was carried out using an appropriate suspended Ubbelohde viscometer. At 298.15 K (room temperature), the instrument was calibrated with freshly prepared double-distilled water. Methanol was used to purify the viscometer, and the literature values of density and viscosity were considered for the purification process.^{24,25} A perfectly cleaned viscometer instrument was dried with a hot thermostat, placed vertically in a glass-walled thermostat (Bose-Panda instruments Pvt. Ltd.), and filled with the experimental solution. For the calculation of viscosity of the experimental solutions, it is required to record the time taken

when the solution is flowing from the upper mark to the lower mark through the capillary of the viscometer by the force of gravity. Therefore, a solution with high viscosity, which has a very large frictional force within the molecules in solution, takes more time to move the molecules through the capillary tube from the upper mark to the lower one. The viscosities of the solution (η) were calculated using the following equation

$$\eta_r = \frac{\eta}{\eta_0} = \frac{\rho t}{\rho_0 t_0} \quad (1)$$

The absolute viscosities, densities ($\text{g}\cdot\text{cm}^{-3}$), and flow times (s) are denoted as η_0 , η ; ρ , ρ_0 ; and t , t_0 for the experimental solution and the solvent, respectively. The temperature during the experiment was kept up to 0.01 K of the instrument. Time flows during the experiment of the solutions were recorded at thermal equilibrium with a stopwatch, and the correctness of the instrument was ± 0.01 s. The uncertainty of viscosity of the measurement was $\pm 0.2 \times 10^{-3}$ mPa·s.

To determine the refractive index, a digital refractometer Mettler Toledo instrument (model: Refracto 30GS; number: 51324660 from India) was considered for this purpose. In the case of measurement of refractive index, ± 0.0002 units approximately was the accuracy of the measurement. The calibration of the refractometer was done by taking distilled water twice for the studied solutions for the accuracy of the measurements. The repeating of calibration was done after a few seconds of each measurement of the refractometer instrument.²³ A light-emitting diode, having wavelength $\lambda = 589.3$ nm, was the source of light of this system. The reading of the measurement of the refractive indices was recorded by taking three or four drops of the sample onto the measurement cell. Since the values of refractive indices depend on the temperature and concentration, we can obtain the refractive index values desired by the user at various temperatures and various concentrations. The solution temperature remained persistent throughout the experiment of the solutions in a Brookfield Digital TC-500 thermostatic water bath (Model: TC-550AP).

We used the Mettler Toledo Instrument (model: In Lab730 probe cell) to determine the solution's conductivity accurately. The great advantage of this cell is that it has the capacity to perform conductivity measurements in the range of 0.01–1000 mS/cm. The cell constant of type 4 graphite cells was 0.56 cm^{-1} for the measurement of conductivity of the studied systems. For the calibration of the using cell here, a freshly prepared solution of 0.01 N concentration of NaCl was used for the experiment. The accuracy of the conductivity measurement was $\pm 0.5\%$. The accuracy of the conductance measurement was $\pm 0.5\%$. The determination of specific conductance of six different concentrations (0.0010, 0.0025, 0.0040, 0.0055, 0.0070, and 0.0085) m of solution was reported at three temperatures. Here, the mentioned symbol "m" signifies the molality of the solution. kg mol^{-1} denotes the unit of molality. The conversion of specific conductance into molar conductance can be performed with the help of the equation $\Lambda = 1000 \kappa/c$, where c signifies the molar concentration of amino acid in the presence of ionic liquid solutions and κ symbolizes the specific conductance of the experimental solutions.^{26,27}

The K9 digital tensiometer (model: K9, KrussGmbH, Hamburg, Germany) was used to evaluate the surface tension of the studied solutions by means of the platinum ring

detachment technique at 298 K. The precision of this tensiometer instrument is very good, and a solid and vibration-free base is present in this instrument. This instrument put on such a place those same demands on its neighbor as a laboratory balance with a resolution of 0.1 mg. The ring is immersed by moving it below the interface of the liquid container. After immersion of the ring into the liquid, the ring was gradually pulled through the intersection, and a meniscus of liquid was formed. It is very crucial for the measurement of surface tension to obtain an accurate value, and a clean and dust-free atmosphere is required. Circulating autothermostatic water was used to maintain the temperature of this device during the experiment of the specified solutions. The solutions were taken in a double-wall glass vessel for the experiment of these solutions. The accuracy of the measurement of this device was $\pm 0.1 \text{ mN m}^{-1}$. Using doubly distilled water, calibration was carried out in the digital K9 tensiometer (Kruss, Germany).

Fourier transformation infrared (FTIR) spectra were taken using the Perkin Elmer spectrometer, Spectrum RXI, with a resolution of 4 cm^{-1} by the disk method at room temperature. The basic principle of this technique is to identify the different functional groups in the molecules and interaction consisting of different functional groups of mixtures. When a specific wavelength source of light is exposed to the compound, the functional group undergoes vibration in different ways such as stretching and bending. In general, the spectrum of a molecule is obtained in the wavenumber range of $(4000\text{--}400) \text{ cm}^{-1}$. KBr is used as a spectrum since it acts as a carrier to the sample and fixes the sample in a cleaner film for FTIR measurement.

The NMR spectroscopic technique gives an idea about the magnetic field induced around different nuclei of the atom in molecules. In the presence of a magnetic field, the sample nuclei undergo excitation in the radio waves, and these waves are readily converted into nuclear magnetic resonance, which can be noted from the NMR signal. The variety of electronic structures and the functional groups in a molecule can be determined from the resonance frequency obtained by an intramolecular magnetic field. This field is highly suitable for characterizing different compounds. In modern organic chemistry, not only monomolecular organic compounds but also other different proteins and complex systems can be identified by the NMR technique. In-depth information about the nature of dynamic, structure, state of reaction, and chemical environment around the molecules can also be obtained from the NMR study.

For the determination of $^1\text{H-NMR}$ spectra, nuclear magnetic resonance (NMR) measurements in the solution state were performed in the D_2O solvent at 298.15 K. In the case of spectral determination, an NMR spectrometer (model: Bruker AVANCE DRX 400 NMR) was used operating at 400 MHz frequency. Signals were denoted as δ values in ppm using residual protonated solvent signals used as internal standards (D_2O : 4.79 ppm). The changes in chemical shift values were noted to analyze the interaction between AA and IL molecules. δ units (ppm) are used for the measurement of chemical shifts of protons. The peak pick facility technique was used to obtain the different peaks of interest using chemical shift values. The uncertainty of δ units was estimated to be better than 0.0005 ppm.¹³

A JASCO (model: V-530) UV–vis spectrophotometer was used to record the UV–visible spectra of experimental solutions of different concentrations. The basic principle of

Table 2. Values of Limiting Apparent Molar Volumes (Φ_V^0), Limiting Molar Refraction (R_M^0), Experimental Slopes (S_V^*), and Viscosity B -Coefficients of (*L*-Methionine + Aq. BTMAC) Systems in Different Molalities (0.001, 0.003, 0.005) of Aqueous Ionic Liquids at Various Working Temperatures and Pressure at 1.013 bar^a

temperature/K	$\Phi_V^0 \times 10^6/\text{m}^3\cdot\text{mol}^{-1}$	R_M^0	$S_V^* \times 10^6/\text{m}^3\cdot\text{mol}^{-2}\cdot\text{kg}$	$B/\text{dm}^3\cdot\text{mol}^{-1}$
		0.001 <i>m</i> IL		
298.15	109.17 ± 0.02	30.5990	−971.58 ± 0.01	5.270 ± 0.034
303.15	111.03 ± 0.04	30.5690	−1203.30 ± 0.05	6.050 ± 0.016
308.15	112.28 ± 0.03	30.5840	−1450.20 ± 0.07	7.070 ± 0.013
		0.003 <i>m</i> IL		
298.15	119.83 ± 0.02	30.5750	−2246.50 ± 0.01	5.448 ± 0.033
303.15	121.70 ± 0.02	30.5790	−2365.60 ± 0.06	6.198 ± 0.027
308.15	122.50 ± 0.03	30.6000	−2421.00 ± 0.09	7.163 ± 0.040
		0.005 <i>m</i> IL		
298.15	125.87 ± 0.02	30.5840	−3000.00 ± 0.08	5.576 ± 0.064
303.15	129.01 ± 0.04	30.5930	−3151.30 ± 0.04	6.315 ± 0.053
308.15	130.68 ± 0.03	30.6090	−3577.40 ± 0.03	7.288 ± 0.035

^aStandard uncertainty in T , $u(T) = \pm 0.01$ K, and in R_M , $u(R_M) = \pm 0.0002$ (confidence level of the measurements is 0.68). # Considering the purity of mass of the chemicals, the combined standard uncertainty in molality is expected to be ± 0.0147 mol·kg^{−1}. * The mixture of water and IL is considered a solvent (kg^{−1}), and this has been expressed as molality.

Table 3. Values of Limiting Apparent Molar Volumes (Φ_V^0), Limiting Molar Refraction (R_M^0), Experimental Slopes (S_V^*), and Viscosity B -Coefficients of (*L*-Methionine + Aq. BTEAC) Systems in Different Molalities (0.001, 0.003, 0.005) of Aqueous Ionic Liquid at Various Working Temperatures and Pressure at 1.013 Bar^a

temperature/K	$\Phi_V^0 \times 10^6/\text{m}^3\cdot\text{mol}^{-1}$	R_M^0	$S_V^* \times 10^6/\text{m}^3\cdot\text{mol}^{-2}\cdot\text{kg}$	$B/\text{dm}^3\cdot\text{mol}^{-1}$
		0.001 <i>m</i> IL		
298.15	109.66 ± 0.02	30.5690	−1165.10 ± 0.03	5.305 ± 0.039
303.15	111.67 ± 0.05	30.6070	−1251.10 ± 0.03	6.094 ± 0.067
308.15	112.76 ± 0.05	30.6440	−1527.60 ± 0.01	7.099 ± 0.020
		0.003 <i>m</i> IL		
298.15	120.17 ± 0.05	30.5830	−2358.50 ± 0.05	5.496 ± 0.052
303.15	122.21 ± 0.04	30.6230	−2447.90 ± 0.03	6.226 ± 0.038
308.15	123.01 ± 0.05	30.6720	−2503.70 ± 0.04	7.202 ± 0.034
		0.005 <i>m</i> IL		
298.15	127.59 ± 0.05	30.6120	−2936.00 ± 0.01	5.628 ± 0.059
303.15	130.83 ± 0.04	30.6510	−3561.90 ± 0.00	6.359 ± 0.054
308.15	132.23 ± 0.05	30.6950	−3598.80 ± 0.02	7.345 ± 0.071

^aStandard uncertainty in T , $u(T) = \pm 0.01$ K, and in R_M , $u(R_M) = \pm 0.0002$ (confidence level of the measurements is 0.68). # Considering the purity of mass of the chemicals, the combined standard uncertainty in molality is expected to be ± 0.0147 mol·kg^{−1}. * The mixture of water and IL is considered a solvent (kg^{−1}), and this has been expressed as molality.

the UV–visible technique is that the UV light is absorbed by the studied sample giving rise to its distinct UV–spectra. In this technique, two kinds of lamps are taken as sources of light, one is a deuterium lamp for the UV–visible range (170–380 nm) and the other is a tungsten lamp for the visible and near-infrared ranges (380–780 nm and 780–3300 nm, respectively), which are used as single sources of spectrometers. The accuracy of the wavelength of this spectrophotometer was ± 0.5 nm. A digital thermostat was used during the experiment, and the temperature of the cell was maintained from 298.15 to 308.15 K.

For minimization of loss of evaporation, sufficient fortifications were taken throughout the actual measurements. For determination of mass measurements, a digital electronic analytical balance (model: Mettler Toledo, AG 285, from Switzerland) was used for stock solutions with a precision of $\pm 0.0003 \times 10^{-3}$ kg. According to mass purity of the chemicals, the combined standard uncertainty in molality is expected to be ± 0.0147 mol·kg^{−1}.

The following formula was used for the conversion of molality into molality using experimental density values.²⁸

$$m = \frac{1}{(\rho/c) - (M/1000)} \quad (2)$$

2.3. Computational Details. All of the calculations obtained by the density functional theory (DFT) were performed utilizing the Gaussian 16 program.²⁹ Ground-state geometry optimizations of *L*-methionine, ionic liquids, and the composites were performed at the B3LYP/6-31+G(d) level of theory. In the course of ground-state optimization, solvent effects (water) were introduced employing the polarizable continuum model (PCM) applying the integral equation formalism (IEF) variant by the Gaussian 16 package. To check whether the energy-minimized geometries correspond to the true ground-state geometries, vibration frequency analyses were performed at the same level of theory. No imaginary frequency confirms that the geometries are minima on the potential energy surfaces. Meanwhile, the different kinds of weak forces like van der Waals interactions, H-bonding, and steric interactions were investigated by noncovalent interaction (NCI) index plots of the reduced density gradient (RDG)³⁰ using the Multiwfn 3.7 suite.³¹ Furthermore, molecular electrostatic potential (MESP) maps were visualized at

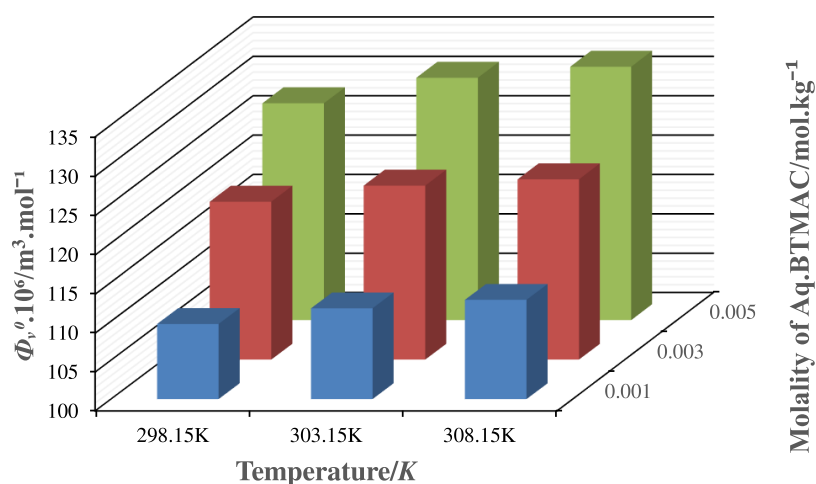


Figure 1. Variation of Φ_v^0 of L-methionine as a working temperature (T/K) and various concentrations of aqueous BTMAC solutions.

ground-state geometries to understand the type and moieties involved in the interactions. Finally, by utilizing the following formula, adsorption energies, ΔE_{ads} ($\text{kJ}\cdot\text{mol}^{-1}$), for all of the composite systems were calculated

$$\Delta E_{\text{ads}} = E_{\text{IL-L-methionine}} - E_{\text{IL}} - E_{\text{L-methionine}}$$

where $E_{\text{IL-L-methionine}}$, E_{IL} , and $E_{\text{L-methionine}}$ are the total energies of the geometry optimized complexes, free IL, and L-methionine molecules, respectively.

3. RESULTS AND DISCUSSION

Here, the listed Tables S1 and S2 describe the different physicochemical parameters such as density (ρ), viscosity (η), and molar refraction (R_M) at 298.15, 303.15, and 308.15 K of binary solutions of different molality (m) values of aqueous ionic liquids (BTMAC and BTEAC). Measurements of the refractive index (n_D) and specific conductance (κ) at three temperatures of binary solutions at different molality (m) values of the aqueous ionic liquids (BTMAC and BTEAC) are listed in Tables S3 and S4. The experimental measurements of density, viscosity, and molar refraction of six various sets of concentrations of L-methionine solutions in 0.001, 0.003, and 0.005 molality aqueous IL solutions at various temperatures are mentioned in Tables S5 and S6.

3.1. Density. Volumetric properties such as Φ_v and Φ_v^0 are significant parameters to be considered irrespective of whether or not the interactions are taking place in solution systems. The apparent molar volume Φ_v provides information about the total geometrical volume obtained from the solute and the volume change in the solvent due to contact with the solute molecule around the periphery or cosphere. Tables 2 and 3 show the different parameters such as (Φ_v^0), (R_M^0), (S_V^*), and viscosity B -coefficients of the L-methionine solution in two aqueous ionic liquids at different functions of temperatures.

Considering the densities of solution, we can obtain the value of Φ_v very easily by applying the following given equation,³² and the results are provided in Tables S7 and S8.

$$\Phi_v = M/\rho_0 - (\rho - \rho_0)/m\rho\rho_0 \quad (3)$$

where M signifies the molar mass (g) of the solute, m is the molality ($\text{mol}\cdot\text{kg}^{-1}$) of the solution, and ρ and ρ_0 are the densities ($\text{g}\cdot\text{cm}^{-3}$) of the solution and solvent, respectively. It was found from the results of Φ_v that all values are positive, and they decrease with the increase in concentration (molality)

of (L-methionine + BTMAC + H_2O) and (L-methionine + BTEAC + H_2O) solutions. Conversely, Φ_v values increase with the increase in temperature at all concentrations of L-asparagine and L-glutamine as well. It was also noticed that Φ_v values increase with increasing values of molality (from 0.001 to 0.005) of aqueous BTEAC solutions simultaneously. It was further observed from the above volumetric results that the values of Φ_v of L-methionine solutions in BTEAC ionic liquids are higher than those of L-methionine in BTMAC ionic liquids.

Knowledge acquired from limiting the apparent molar volume (Φ_v^0) is a very important parameter to analyze the interactions happening in solution. Evaluation of limiting apparent molar volumes (Φ_v^0) was carried out using eq 4³³ obtained from the plots of Φ_v versus m by a least-squares treatment.

$$\Phi_v = \Phi_v^0 + S_V^* m \quad (4)$$

where Φ_v^0 is the limiting apparent molar volume ($\text{m}^3\cdot\text{mol}^{-1}$) at infinite dilution and S_V^* ($\text{m}^3\cdot\text{mol}^{-2}\cdot\text{kg}$) denotes the experimental slope, which is considered as a pairwise volumetric virial coefficient. The physical significance of S_V^* indicates the solute–solute interactions among the amino acids. A small value of S_V^* indicates a higher value of interaction among the amino acids. Here, we observe the variation of Φ_v^0 values of L-methionine solutions at various concentrations of ILs at three temperatures. It was found from the above-listed table that the Φ_v^0 values are all positive, and these values are found to increase on changing the concentration and temperature of the solutions of L-methionine as well as on changing the concentrations of aqueous ionic liquids. The above-mentioned results of Φ_v^0 , which were in agreement with previous literature values;¹⁰ here, the Φ_v^0 values of L-methionine in aqueous ionic liquid (BTMAC) solutions are lower compared with BTEAC ionic liquids under any circumstance.

A similar type of relationship has been identified previously for the homologous sequence of amino acids in electrolyte solutions in an aqueous medium.^{34,35} The values of S_V^* are all negative, and simultaneously, these values decrease with an increase in molality of the solutions, and the same approaches are found in the case of temperature. Furthermore, it is observed that BTEAC has lower S_V^* values than BTMAC.

The magnitude of the solute–solvent interaction depends on the magnitude of Φ_v^0 values. From Tables 2 and 3, we

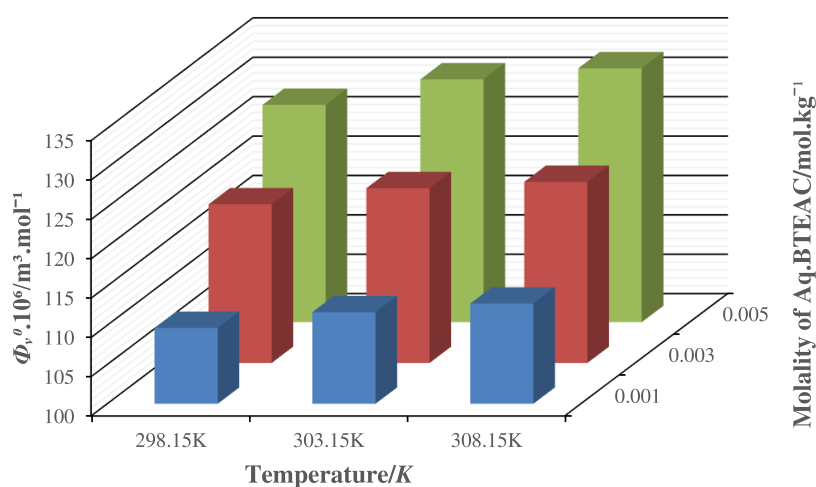


Figure 2. Variation of Φ_v^0 of L-methionine as a working temperature (T/K) and various concentrations of aqueous BTEAC solutions.

Table 4. Values of Empirical Coefficient (a_0 , a_1 , and a_2) of (L-Methionine + Aq. BTMAC) and (L-Methionine + Aq. BTEAC) Systems in Different Molalities of ILs (BTMAC) and (BTEAC) at Various Working Temperatures and Pressures at 1.013 Bar^a

different molalities of aq. ILs solutions/mol·kg ⁻¹	L-Methionine in BTMAC			L-Methionine in BTEAC		
	$a_0 \times 10^6/\text{m}^3 \cdot \text{mol}^{-1}$	$a_1 \times 10^6/\text{m}^3 \cdot \text{mol}^{-1} \cdot \text{K}^{-1}$	$a_2 \times 10^6/\text{m}^3 \cdot \text{mol}^{-1} \cdot \text{K}^{-2}$	$a_0 \times 10^6/\text{m}^3 \cdot \text{mol}^{-1}$	$a_1 \times 10^6/\text{m}^3 \cdot \text{mol}^{-1} \cdot \text{K}^{-1}$	$a_2 \times 10^6/\text{m}^3 \cdot \text{mol}^{-1} \cdot \text{K}^{-2}$
	298.15 K	303.15 K	308.15 K	298.15 K	303.15 K	308.15 K
0.001	-1104.4	7.708	-0.0122	-1673.3	11.466	-0.0184
0.003	-1925.9	13.242	-0.0214	-2243.0	15.320	-0.0248
0.005	-2718.7	18.306	-0.0294	-3391.7	22.776	-0.0368

^aStandard uncertainty in T and $u(T) = \pm 0.01$ K (confidence level of the measurements is 0.68). # Considering the purity of mass of the chemicals, the combined standard uncertainty in molality is expected to be ± 0.0147 mol·kg⁻¹. * The mixture of water and IL is considered the solvent (kg⁻¹), and this has been expressed as molality.

obtained the Φ_v^0 values for both systems, and it was observed that all are positive and it is maximum for L-Met in the 0.005m BTEAC system at 308.15 K, and the minimum was found for L-Met in the 0.001m BTMAC system at 298.15 K. Thus, maximum interactions were found in the former case, minimum interactions were found in the latter case between AA and ILS, and similar types of explanation are obtained from Figures 1 and 2 respectively. Based on the positive values of Φ_v^0 obtained from the (L-methionine + Aq. glucose solutions) system,¹⁰ the interaction phenomenon between the solute and the solvent was explained, which has similar trends with the solute–solvent interaction in L-methionine with BTMAC and BTEAC. The most probable reason is that during the interaction occurring between the solute and the solvent, solvent molecules are released from the movable solvation layers.²⁸ It has been found from Tables 2 and 3 that the values of Φ_v^0 of L-methionine in the aqueous BTEAC ionic liquid were higher than in the aqueous BTMAC ionic liquid at all molalities and temperatures, indicating that under all existing conditions the maximum interaction was found in the (Aq. BTEAC + L-methionine) system compared with the other system. On the contrary, S_V^* indicates the magnitude of solute–solute interaction, which has a negative sign and a pairwise interaction dominant by the interaction of the hydrophobic part of the ionic liquid with the hydrophobic part of the amino acid. It can be seen from Tables 2 and 3 that the values of S_V^* are very less compared with Φ_v^0 , indicating that the solute–solute interaction is very poor and the values of S_V^* decrease with an increase in temperature and molality of the ionic liquid, suggesting that the strength of L-methionine

with water is decreasing. The values of S_V^* suggest that the highest degree of interaction among solutes was found in the L-Met 0.001m BTMAC solution at 298.15 K and the minimum was found in the 0.005m BTEAC solution at 308.15 K. It is also notified that the L-methionine–L-methionine interaction in BTMAC was found to be better than the corresponding solution in BTEAC, which can be explained by the higher values of S_V^* that are listed in Tables 2 and 3. It seems that the orientation of the small hydrophobic portion ($-\text{CH}_3$) of BTMAC is lower than the higher hydrophobic portion ($-\text{CH}_2-\text{CH}_3$) of the BTEAC ionic liquid, which has been shown by their molecular structures in Scheme 1. Thus, the main reason for the hydrophobic–hydrophobic interactions becomes stronger for longer alkyl ($-\text{CH}_2-\text{CH}_3$) chains of BTEAC with the alkyl chain of amino acid (L-methionine).

Considering the comparison of the two systems (L-Met + Aq. BTMAC) and (L-Met + Aq. BTEAC) in magnitude of Φ_v^0 quantitatively, we see that the values of S_V^* are very small compared to the Φ_v^0 values for the above-mentioned two systems. The above-mentioned explanation suggested that the molecular interaction behavior of L-Met with ionic liquid (BTMAC and BTEAC) dominates over L-Met with L-Met in all cases of solutions.^{33,36} The resultant volume contractions that occurred in the systems echo the hydrophobic interactions in the amino acids by the caging effect of the water molecule or hydrophobic hydration.³⁷ Values from previous literature show that similar types of links have been identified for homologous series of amino acids in electrolyte solutions in an aqueous medium.³⁵

Table 5. Values of Limiting Molar Expansibilities (Φ_E^0) for the (L-Methionine + Aq. BTMAC) System in Ionic Liquid at Various Temperatures and Pressures at 1.013 Bar^a

molality of aq. IL soln. (mol·kg ⁻¹)	$\Phi_E^0 \times 10^6/\text{m}^3\cdot\text{mol}^{-1}\cdot\text{K}^{-1}$			$(\delta\Phi_E^0/\delta T)_p \times 10^6/\text{m}^3\cdot\text{mol}^{-1}\cdot\text{K}^{-2}$
	298.15 K	303.15 K	308.15 K	
0.001	0.4330	0.3110	0.1890	-0.0244
0.003	0.4812	0.2672	0.0532	-0.0428
0.005	0.7748	0.4808	0.1868	-0.0588

^aStandard uncertainty in T and $u(T) = \pm 0.01$ K (confidence level of the measurements is 0.68). # Considering the purity of mass of the chemicals, the combined standard uncertainty in molality is expected to be ± 0.0147 mol·kg⁻¹. * The mixture of water and IL is considered the solvent (kg⁻¹), and this has been expressed as molality.

Table 6. Values of Limiting Molar Expansibilities (Φ_E^0) for the (L-Methionine + Aq. BTEAC) Solution in IL (BTEAC) at Different Temperatures and Pressures at 1.013 Bar^a

molality of aq. IL soln. (mol·kg ⁻¹)	$\Phi_E^0 \times 10^6/\text{m}^3\cdot\text{mol}^{-1}\cdot\text{K}^{-1}$			$(\delta\Phi_E^0/\delta T)_p \times 10^6/\text{m}^3\cdot\text{mol}^{-1}\cdot\text{K}^{-2}$
	298.15 K	303.15 K	308.15 K	
0.001	0.4941	0.3101	0.1261	-0.0368
0.003	0.5318	0.2838	0.0358	-0.0496
0.005	0.8322	0.4642	0.0962	-0.0736

^aStandard uncertainty in T and $u(T) = \pm 0.01$ K (confidence level of the measurements is 0.68). # Considering the purity of mass of the chemicals, the combined standard uncertainty in molality is expected to be ± 0.0147 mol·kg⁻¹. * The mixture of water and IL is considered the solvent (kg⁻¹), and this has been expressed as molality.

The value of Φ_v^0 depends on the temperature, and these values were calculated using the following polynomial equation at three temperatures separately.³⁸

$$\Phi_v^0 = a_0 + a_1T + a_2T^2 \quad (5)$$

where $a_0/\text{m}^3\cdot\text{mol}^{-1}$, $a_1/\text{m}^3\cdot\text{mol}^{-1}\cdot\text{K}^{-1}$, and $a_2/\text{m}^3\cdot\text{mol}^{-1}\cdot\text{K}^{-2}$ are empirical coefficients. These values depend on the nature of the solute and the molality of the cosolvent, whereas T denotes the temperature in the Kelvin scale.

Descriptions of empirical coefficient values (a_0 , a_1 , and a_2) of (L-Met + Aq. BTMAC) and (L-Met + Aq. BTEAC) systems at three temperatures in different concentrations (molalities) of two aqueous ionic liquids are listed in Table 4. The values of limiting apparent molar expansibilities (Φ_E^0) were calculated using the first derivative of eq 5 of (L-Met + Aq. BTMAC) and (L-Met + Aq. BTEAC) systems in aqueous ILs solutions at various temperatures and are listed in Tables 5 and 6.

$$\Phi_E^0 = (\delta\Phi_v^0/\delta T)_p = a_1 + 2a_2T \quad (6)$$

The values of $(\Phi_E^0)/\text{m}^3\cdot\text{mol}^{-1}\cdot\text{K}^{-1}$ for all of the systems are found to be positive in both ionic liquid solutions, which indicates that the probability of caging or packing effect of both systems is absent. The interaction acts as a structure-breaker or synergistic structure-maker of the studied system. In this regard, in the solution phase, Hepler developed a concept to establish a mode to study the solute–solvent interaction.³⁹ The probability of making the structure-breaker or structure-maker interaction between the solute and the solvent also depends on the values of $(\delta\Phi_E^0/\delta T)_p/\text{m}^3\cdot\text{mol}^{-1}\cdot\text{K}^{-2}$ according to the Hepler opinion⁴⁰

$$(\delta\Phi_E^0/\delta T)_p = (\delta^2\Phi_v^0/\delta T^2)_p = 2a_2 \quad (7)$$

It is common knowledge that the solutes that make the structure with the solvent should have positive values of $(\delta\Phi_E^0/\delta T)_p$, whereas those that break the structure with the solvent should have negative values of $(\delta\Phi_E^0/\delta T)_p$.

Here, the negative values obtained from the calculation by the above expression (eq 7) are listed in Tables 5 and 6. We

note from Tables 5 and 6 that the probability of the solute–solvent interaction at various temperatures between (L-methionine + Aq. BTMAC) and (L-methionine + Aq. BTEAC) is structure-breaking and the maximum disruption of the solvent molecule by the solute molecule is observed in the case of L-methionine with Aq. BTEAC, and it has also been observed that the probability of solvent disruption by the solute increases with the molality of the ionic liquid and temperature. The highest packing or caging effect is observed for the highest concentration of IL (BTEAC) and the highest working temperature among all of the concentrations and all of the working temperatures.

3.2. Viscosity. In aqueous electrolytic solutions, the degree of hydration of an ion and structural interactions^{41,42} within the hydration of ionic cospheres⁴² can be explored easily by studying the viscosity coefficient with varying concentrations and temperatures of solution. The results of viscosity values are listed in Tables S1 and S2. It has been observed from the listed table that the values of viscosity of different concentrations of solutions increase with increasing molality of the ILs. Analogous results have been reported for other amino acids.⁶ The solute–solvent interaction between L-Met in an aqueous solution of glucose,¹⁰ elucidated on depending upon the values of B -coefficient which has quite different in values of viscosity coefficient but similar trends of nature of interaction of solute–solvent in L-Methionine with BTMAC and BTEAC.

The above-mentioned fact can be explained well based on collision theory. According to this theory, on increasing the molecular number, the molecular collision increases, as a result of which the molecules lose kinetic energy. Here, on increasing the molality of the ionic liquid, the molecular number of the ionic liquid in solution further increases; therefore, there is loss of kinetic energy in the system due to an increase in the collision number among the molecules in solution. As a consequence, the molecules prefer to stick among themselves with increasing viscosity.

In the case of a nonelectrolytic system, the Jones–Dole equation was used to analyze the viscosity data obtained from

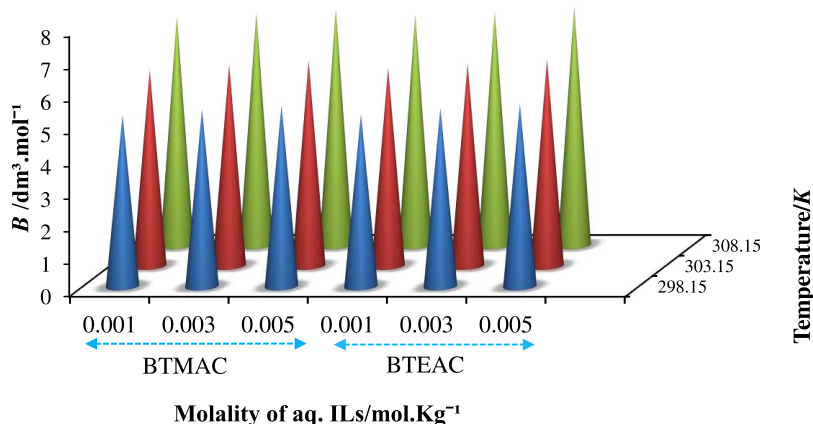


Figure 3. *B*-coefficient plot of *L*-methionine as a function of various temperatures (*T*/K) and various concentrations of aqueous BTMAC (IL) and BTEAC (IL) solutions.

the measurements of viscosity (where the *A*-coefficient, reflecting interionic interactions, is 0)^{43,44}

$$\eta/\eta^0 - 1 = Bc \quad (8)$$

Here, η and η^0 are viscosities of the solution and the solvent, respectively, and c is the concentration of the solution in molarity ($\text{mol}\cdot\text{L}^{-1}$).

The viscosity *B*-coefficient/ $\text{dm}^3\cdot\text{mol}^{-1}$ denotes a parameter known as the adjustable parameter, which is a measure of the effective hydrodynamic volume, which in turn determines the interaction between the solute and the solvent in the mixed medium. The value of the viscosity *B*-coefficient depends on not only the structural information of the ions but also the partial molar entropies of the ions remaining in the solution phase. According to the Jones–Dole equation, using the plots of $\eta/\eta^0 - 1$ vs c , the viscosity *B*-coefficients achieved by the linear least-square analysis are described in Tables 2 and 3 for *L*-Met solutions in BTMAC and BTEAC aqueous ionic liquids at three different temperatures and pressure at 1.013 bar, respectively. Figure 3 suggests the change of *B*-values of *L*-methionine in BTMAC and BTEAC against different concentrations (0.001, 0.003, and 0.005 molality) of ionic liquid solutions at various temperatures, which showed similar trends to previous literature values.¹⁰

Viscosity *B*-coefficients, which are empirical constants, are used to describe the solute and solvent interaction phenomenon in the studied mixed solution, which almost depends on not only the size and shape but also the structural effects of the studied molecules.² It has been noted that in all of the three molalities of an ionic liquid in solution, the viscosity *B*-coefficient values are large enough, which characterize the structural upgradation of a liquid in the presence of an ionic liquid with 0.001, 0.003, and 0.005 molalities; this also supports similar trends of results obtained from the volumetric properties. It can be seen from Tables 2 and 3 that all of the values of the *B*-coefficient are positive, thus suggesting that the interactions of the solute with the solvent are strong. On increasing the viscosity value of the solvent, the strength of the interactions of the studied systems also increases, which is in accordance with the conclusions obtained from the limiting apparent molar volume (Φ_v^0) in an earlier section. Due to the presence of solute molecules around the solvent molecules,

solute–solvent interactions take place to a large extent in solutions.

The solute molecules are solvated all around by associating with solvent molecules by the solute–solvent interactions,⁴⁵ and this is the main reason for the larger viscosity *B*-coefficient values.

Furthermore, interactions associated with the solute and solvent are reinforced with increasing temperatures as well as an increase in concentration (0.001–0.005 molality) of aqueous solutions of IL. The interaction becomes more in the case of *L*-methionine in BTEAC compared with *L*-methionine in an aqueous solution of the BTEAC ionic liquid. In this system, the water molecules are replaced by their surrounding cosolvent molecules from the sphere of the solvation layer, which brings them closer to the solute and solvent; as a result, viscosity *B*-coefficients are increased, which account for the strongest interactions among the solute and the solvent molecule. Their replacement of water molecules by more cosolvent molecules from the solvation sphere brings the solute and cosolvent closer, thereby increasing the viscosity *B*-coefficients, and accounts for the higher solute–solvent interaction. Viscometric calculations indicate that the viscosity *B*-coefficient values are all positive, suggesting the less predominant nature of the solute–solute interaction compared with the solute–solvent interaction.

The interactions between the solute and solvent function as a structure-maker or structure-breaker that depends upon the ratio of dB/dT (first derivative of the viscosity *B*-coefficient over temperature). According to the Eyring viscosity theory, the dB/dT has a negative value, which signifies that the measurement of activation energy required for the viscous flow is higher in solution than in the pure solvent.^{35,46,47} Variations of viscosity *B*-coefficients of *L*-methionine with dB/dT values in various molalities (0.001, 0.003, 0.005) of studied ionic liquids at various temperatures are given in Tables 7 and 8. The phenomenon of the kosmotropic effect, i.e., the structure-making effect, depends on the negative sign of dB/dT values of the system, whereas the chaotropic effect, i.e., the structure-breaking effect, depends on the positive sign of dB/dT values. Tables 7 and 8 show that all of the dB/dT values of the two ionic liquid systems are positive, indicating that the amino acid, *L*-Met, acts as a structure-breaker in the solution. Similar trends of results were found in the literature.²⁸

Table 7. Viscosity B-Coefficients and dB/dT Values of the (L-Methionine + Aq. BTMAC) System in Various Concentrations of the BTMAC Ionic Liquid at Various Temperatures and Pressures at 1.013 Bar^a

T/K	0.001m IL	0.003m IL	0.005m IL	dB/dT
	B	B	B	
298.15 K	5.270	5.448	5.576	0.180
303.15 K	6.050	6.198	6.315	0.171
308.15 K	7.070	7.163	7.288	0.171

^aStandard uncertainty in T and $u(T) = \pm 0.01$ K (confidence level of the measurements is 0.68). # Considering the purity of mass of the chemicals, the combined standard uncertainty in molality is expected to be ± 0.0147 mol·kg⁻¹. * The mixture of water and IL is considered the solvent (kg⁻¹), and this has been expressed as molality.

Table 8. Viscosity B-Coefficients and dB/dT Values of the (L-Methionine + Aq. BTEAC) System in Various Concentrations of the BTEAC Ionic Liquid at Various Temperatures and Pressures at 1.013 Bar^a

T/K	0.001m IL	0.003m IL	0.005m IL	dB/dT
	B	B	B	
298.15 K	5.305	5.496	5.628	0.179
303.15 K	6.094	6.226	6.359	0.170
308.15 K	7.099	7.202	7.345	0.171

^aStandard uncertainty in T and $u(T) = \pm 0.01$ K (confidence level of the measurements is 0.68). # Considering the purity of mass of the chemicals, the combined standard uncertainty in molality is expected to be ± 0.0147 mol·kg⁻¹. * The mixture of water and IL is considered as the solvent (kg⁻¹), and this has been expressed as molality.

The data of viscosity are discussed according to the transition-state theory of relative viscosity proposed by Eyring and co-workers,⁴⁸ which provides information on $\Delta\mu_1^{0\#}$. The following equation has been used to calculate the free activation energy of the solvent molecule of viscous flow per mole

$$\eta_0 = \frac{hN}{V_1^0} \exp\left(\frac{\Delta\mu_1^{0\#}}{RT}\right) \quad (9)$$

Here, h is the Planck constant, N is the Avogadro number, and V_1^0 is the partial molar volume (m³·mol⁻¹) of solvents. We obtain the following form of equation by rearranging the above-mentioned expression (eq 9)

$$\Delta\mu_1^{0\#} = RT \ln(\eta_0 V_1^0 / hN) \quad (10)$$

Based on the treatment of the transition state, Feakins et al. have suggested the following expression, considering the relative viscosity of an electrolytic solution^{49,50}

$$B = (V_1^0 - V_2^0)/1000 + V_1^0(\Delta\mu_1^{0\#} - \Delta\mu_2^{0\#})/1000RT \quad (11)$$

Here, V_2^0 is the partial molar volume of the solute that is present in the solution and $\Delta\mu_2^{0\#}$ is the free activation energy (kJ·mol⁻¹) of viscous flow at infinite dilution per mole of solute. We get eq 12 by rearranging the above eq 11

$$\Delta\mu_2^{0\#} = \Delta\mu_1^{0\#} + \frac{RT}{V_1^0}[B - (V_1^0 - V_2^0)] \quad (12)$$

Considering the transition-state concept, by the viscous flow, the solvent molecules shift very smoothly from the ground state to the transition state. The values of $\Delta\mu_2^{0\#}$ are considered a free energy transfer for the two states (ground state to transition state) of ionic liquids. All values of $\Delta\mu_2^{0\#}$ are positive, and these values are much higher than those of $\Delta\mu_1^{0\#}$ represented in the ground state. Since $\Delta\mu_2^{0\#} > \Delta\mu_1^{0\#}$ for both studied systems, interactions associated with the ground state are much higher compared to those in the transition state; these values are listed in Table 9, which are similar to the results obtained from previous studies.¹⁰ The intermolecular bond distortion and breaking take place normally in the transition state due to the compactness of solute and solvent molecules in the ground state. Moreover, it can be seen in the above-mentioned table that on increasing the concentration of the ionic liquid from 0.001 to 0.005 in the presence of an amino acid (L-methionine), the $\Delta\mu_2^{0\#}$ values gradually

Table 9. Values of $(\bar{V}_1^{T0} - \bar{V}_2^0)$, $\Delta\mu_1^{0\#}$, $\Delta\mu_2^{0\#}$, $T\Delta S_2^{0\#}$, and $\Delta H_2^{0\#}$ for (L-Methionine + Aq. BTMAC) and (L-Methionine + Aq. BTEAC) Systems in the Presence of Various Molalities of Aqueous Solution of ILs at Various Temperatures and Atmospheric Pressure of 1.013 bar^a

parameters	0.001m			0.003m			0.005m		
	T = 298.15 K	303.15 K	308.15 K	T = 298.15 K	303.15 K	308.15 K	298.15 K	303.15 K	308.15 K
L-Met + BTMAC									
$(\bar{V}_1^0 - \bar{V}_2^0)/\text{m}^3\cdot\text{mol}^{-1}$	-94.79	-97.82	-97.29	-110.13	-112.09	-112.86	-119.82	-122.68	-123.66
$\Delta\mu_1^{0\#}/\text{kJ}\cdot\text{mol}^{-1}$	8.91	9.03	9.07	8.95	9.06	9.17	9.01	9.14	9.17
$\Delta\mu_2^{0\#}/\text{kJ}\cdot\text{mol}^{-1}$	634.10	758.47	944.49	665.33	817.07	996.17	710.11	861.49	1027.66
$T\Delta S_2^{0\#}/\text{kJ}\cdot\text{mol}^{-1}$	9254.57	9409.74	9564.97	9863.99	10029.41	10194.83	9467.75	9626.52	9785.30
$\Delta H_2^{0\#}/\text{kJ}\cdot\text{mol}^{-1}$	9888.67	10168.21	10509.46	10529.32	10846.48	11191.00	10177.86	10488.01	10812.96
L-Met + BTEAC									
$(\bar{V}_1^0 - \bar{V}_2^0)/\text{m}^3\cdot\text{mol}^{-1}$	-95.41	-97.83	-99.29	-110.75	-112.78	-113.55	-122.18	-125.85	-127.43
$\Delta\mu_1^{0\#}/\text{kJ}\cdot\text{mol}^{-1}$	8.94	9.07	9.10	8.98	9.12	9.16	9.01	9.14	9.17
$\Delta\mu_2^{0\#}/\text{kJ}\cdot\text{mol}^{-1}$	659.65	802.21	988.98	683.55	836.57	1031.31	729.43	874.52	1053.32
$T\Delta S_2^{0\#}/\text{kJ}\cdot\text{mol}^{-1}$	9664.83	9826.91	9988.99	10368.46	10542.34	10716.22	9653.50	9815.39	9977.28
$\Delta H_2^{0\#}/\text{kJ}\cdot\text{mol}^{-1}$	10324.48	10629.11	10977.97	11052.01	11378.91	11747.53	10382.93	10689.91	11030.60

^aStandard uncertainty in temperature $u(T) = \pm 0.01$ K. # Considering the purity of mass of the chemicals, the combined standard uncertainty in molality is expected to be ± 0.0147 mol·kg⁻¹. * The mixture of water and IL is considered the solvent (kg⁻¹), and this has been expressed as molality.

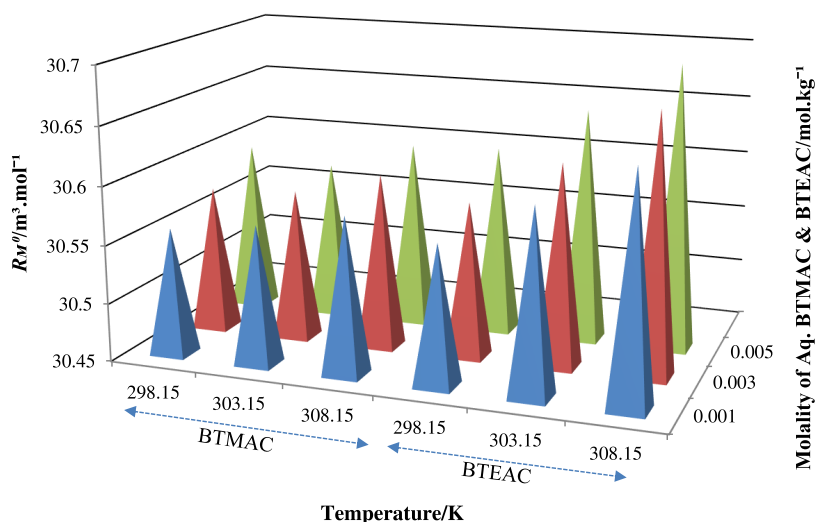


Figure 4. Variation of limiting molar refraction (R_M^0) of *L*-methionine as a function of temperature (T/K) and various concentrations of aqueous BTMAC and BTEAC solutions.

increase. Thus, we can conclude from the values of $\Delta\mu_2^{0\#}$ that a more structured ionic liquid has been found in the ground state. Considering the following equation, we could evaluate the values of $\Delta S_2^{0\#}$, entropy for activation in the (*L*-Met + Aq. BTMAC) and (*L*-Met + Aq. BTEAC) systems, accurately⁵¹

$$d(\Delta\mu_2^{0\#})/dT = -\Delta S_2^{0\#} \quad (13)$$

The negative slope can be observed from the plots of $\Delta\mu_2^{0\#}$ versus T . From this plot, the value of $\Delta S_2^{0\#}$ ($\text{kJ}\cdot\text{mol}^{-1}$) is obtained by the least-squares technique. Enthalpy of activation, ($\Delta H_2^{0\#}$) ($\text{kJ}\cdot\text{mol}^{-1}$), can be calculated from the following relation⁵¹

$$\Delta H_2^{0\#} = \Delta\mu_2^{0\#} + T\Delta S_2^{0\#} \quad (14)$$

$\Delta H_2^{0\#}$ and $\Delta S_2^{0\#}$ values are displayed in Table 9. Since the values of $\Delta\mu_1^{0\#}$ for both systems are almost the same for all of the molalities of ILs, only the viscosity B -coefficient and the limiting molar volume ($\bar{V}_1^0 - \bar{V}_2^0$) are considered important for the determination of values of $\Delta\mu_2^{0\#}$. According to the opinion of Feakins et al.,⁴⁴ the $\Delta\mu_2^{0\#}$ values are much greater than that of $\Delta\mu_1^{0\#}$ for the positive viscosity B -coefficient of the studied solutions, which tells us about the greater interactions between the solute and solvent molecules in the transition state by the rupture and altering of the intermolecular force of interaction associated with the solvent structure.^{52,53} In both systems of studied solutions, it was found that both $\Delta S_2^{0\#}$ and $\Delta H_2^{0\#}$ have positive values, which indicates that bond breaking occurred in the transition-state formation and these values increase accordingly. Actually it is very challenging to assign a particular mechanism for a system, although a very popular model is applied here, which may propose the disorder condition of the slip-plane model.⁵³ At the end, on applying the Feakins et al. model, as $\Delta\mu_2^{0\#} > \Delta\mu_1^{0\#}$, the amino acid (*L*-Met) behaves as a structure-breaker solute. The value of $\Delta\mu_2^{0\#}$ increases on increasing the temperature of the studied system, which also indicates that the solute–solvent interaction increases with rising temperatures. These types of similar results were found from a previous study.¹⁰ This also supports the same characteristics of solutes dB/dT in the presence of both ionic liquids at different molalities.

3.3. Refractive Index. Optical data of the refractive index of the experimental solutions provide important information regarding molecular interactions in terms of molecular structures in the solutions. Refractive index signifies the speed of light, whose value also increases with increasing concentration due to interactions among the components of a system. Measurement of the refractive index (n_D) of the studied systems can provide important information related to interactions associated with the molecules in the solution medium. The Lorentz–Lorenz relation is composition-dependent, and this equation is used to set up a relationship between the refractive index of mixing and molar refractions in a solution. The refractive index (n_D) values of *L*-methionine solutions at different molalities of two ILs are provided in Tables S9 and S10.

The following Lorentz–Lorenz relation was carried out using the value of the refractive index to evaluate the molar refraction R_M ³⁵

$$R_M = \{(n_D^2 - 1)/(n_D^2 + 2)\}(M/\rho) \quad (15)$$

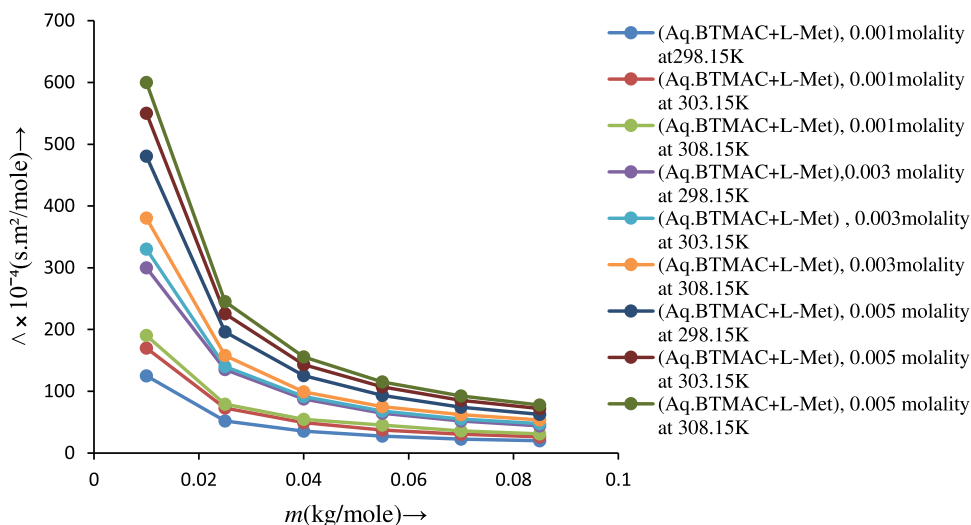
where R_M is the molar refraction, n_D is the refractive index, M is the molar mass (kg) of the solute, and ρ is the density ($\text{kg}\cdot\text{m}^{-3}$) of the solution. The refractive index (n_D) of an element is well-defined as the ratio of the speed of light in vacuum to that in the medium (c_0/c) (where c_0 denotes the speed of light in vacuum and c denotes the speed of light in a medium). To specify the definition of refractive index more simply, n_D of a compound refers to its ability to refract light as it transfers from one medium to another; therefore, if the refractive index (n_D) of a compound is higher, the light is more refracted in the refractometer.⁵⁴ As stated by Deetlefs et al., a more tightly packed system of molecules indicates that the compound is denser and the value of n_D becomes higher.⁵⁵ Thereafter, the refractive index (n_D) of a system signifies the measure of denseness of the studied system.

Here, we note that the refractive index (n_D) values reported in Tables S3–S4 and S9–S10 decrease but the molar refraction (R_M) values (reported in Tables S1 and S2) increase with an increase in temperature. The variation of the two properties (n_D , R_M) with temperature is opposite to each other. However, on increasing the concentrations of AA and IL, the

Table 10. Molar Conductance (Λ) of (L-Methionine + Aq. BTMAC) and (L-Met + Aq. BTEAC) Systems in Aqueous BTMAC and BTEAC Ionic Liquid Solutions in (0.001*m*, 0.003*m*, 0.005*m*) at Various Temperatures and Pressure at 1.013 Bar^a

amino acid concentrations <i>m</i> (mole/kg)	molar conductance of the (L-Methionine + Aq. BTMAC) system $\Lambda \times 10^{-4}$ ($S \cdot m^2 \cdot mol^{-1}$)			molar conductance of the (L-Methionine + Aq. BTEAC) system $\Lambda \times 10^{-4}$ ($S \cdot m^2 \cdot mol^{-1}$)		
	298.15 K	303.15 K	308.15 K	298.15 K	303.15 K	308.15 K
0.001 <i>m</i> IL						
0.0010	125.1	170.0	190.2	110.3	120.0	140.3
0.0025	52.0	73.0	79.0	48.0	53.3	61.0
0.0040	35.5	49.5	54.8	32.5	36.7	42.1
0.0055	27.3	37.2	45.2	25.7	28.5	32.1
0.0070	22.7	30.6	36.1	20.7	24.1	27.3
0.0085	19.9	26.3	31.1	17.8	21.1	24.3
0.003 <i>m</i> IL						
0.0010	300.0	330.3	380.3	290.0	310.7	330.0
0.0025	135.0	140.0	158.0	120.0	129.0	138.3
0.0040	87.5	91.5	99.2	77.6	82.5	88.5
0.0055	64.5	68.0	75.1	57.7	62.4	66.2
0.0070	51.9	55.1	62.3	46.4	50.3	53.1
0.0085	44.0	47.7	53.6	39.3	42.5	45.8
0.005 <i>m</i> IL						
0.0010	480.5	550.3	600.0	470.0	520.1	540.6
0.0025	196.0	225.4	245.1	192.4	213.6	221.0
0.0040	125.5	143.3	155.5	123.0	135.0	140.5
0.0055	93.5	107.0	115.3	90.6	100.7	104.5
0.0070	74.1	85.6	92.3	73.1	80.9	83.3
0.0085	62.6	72.1	77.8	62.1	67.8	71.2

^aStandard uncertainties $u(\Lambda) = 0.5 S \cdot m^2 \cdot mol^{-1}$, * Standard uncertainty in T and $u(T) = \pm 0.01 K$ (confidence level of the measurements is 0.68). # Considering the purity of mass of the chemicals, the combined standard uncertainty in molality is expected to be $\pm 0.0147 mol \cdot kg^{-1}$. * The mixture of water and IL is considered the solvent (kg^{-1}), and this has been expressed as molality.

**Figure 5. Molar conductance (Λ) variation plot vs the concentration of L-methionine in various concentrations of aqueous BTMAC solutions at various temperatures (T/K).**

refractive index and molar refraction (both parameters) also increase in the solution medium.

This observation is quite similar to the results described in the literature for other amino acids (AAs) in aqueous organic electrolyte solutions.⁸¹ However, it is observed from the table that the n_D and R_M values of L-Met in BTEAC have higher values than in BTMAC solutions. This trend of similarity also supports the volumetric and viscometric conclusions attained for the studied system. The tight compactness of the molecules in the solutions depends on the higher value of the refractive

index. Since the refractive index value of the (L-methionine + Aq. BTEAC) system is higher than that of the (L-methionine + Aq. BTMAC) system, it indicates that the (L-methionine + Aq. BTEAC) system is a more tightly packed studied system. The limiting molar refraction (R_M^0) shown in Tables 1 and 2 has been assessed by the following equation

$$R_M = R_M^0 + R_S \sqrt{m} \quad (16)$$

where " m " signifies the molality of the solution and R_M^0 denotes the limiting molar refraction. The significance of R_M^0

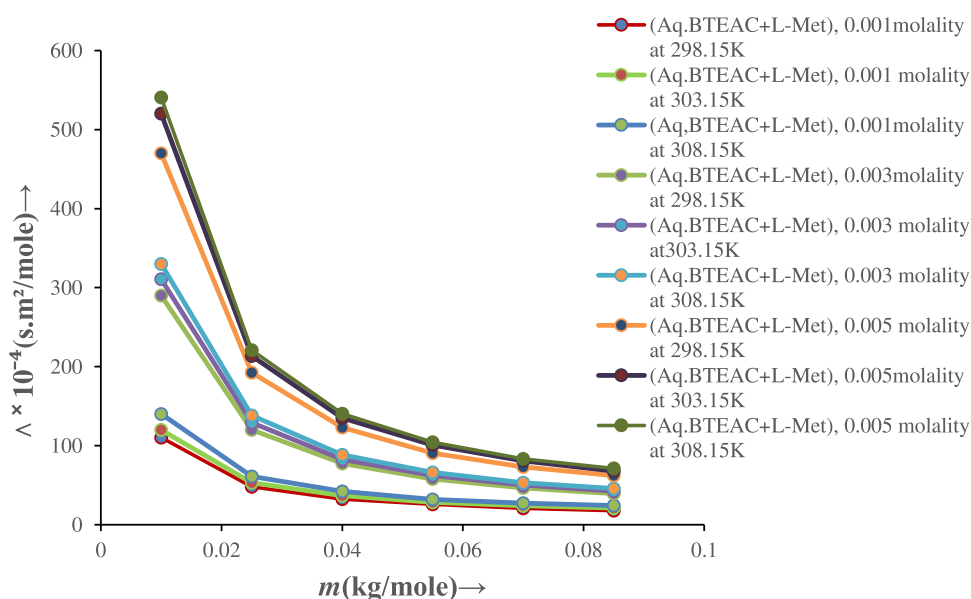


Figure 6. Molar conductance (Λ) variation plot vs concentration of L-methionine in various concentrations of aqueous BTEAC solutions at various temperatures (T/K).

is that it allows us to determine the molecular interactions between a solute and a solvent in a solution medium. A gradual increase of R_M^0 , as mentioned in Figure 4, with rise in molality of the cosolvent (aqueous ionic liquid) and temperature also indicated that the interactions prevailing in the solute and solvent are stronger than the solute and solute interactions. It was found that the value of molar refraction is higher in the case of L-methionine in BTEAC than that of L-methionine in BTMAC, which suggested that the solute–solvent interaction is stronger in the case of L-methionine in BTEAC ionic liquid solutions. Similar types of interactions associated with the solute and solvent molecules were observed in the literature.²⁸ These results obtained in this section are analogous to the calculated limiting apparent molar volume (Φ_v^0) and viscosity B-coefficients values as discussed previously.

3.4. Electrical Conductance. The solute–solvent interactions and the structure-making or structure-breaking propensity of components in a given solvent can be assumed with the help of an electrical conductance study. To explore the properties in a solution, measurement of conductance plays a very crucial role. Here, we have performed the study of conductance of (L-methionine + Aq. BTMAC) and (L-Methionine + BTEAC) systems at various temperatures. The calculation of conductance provides useful information about the interaction properties in the ternary (L-Met + Aq. BTMAC) and (L-Met + Aq. BTEAC) systems.⁵⁶ Here, solute–solute interaction, solute–solvent interaction, and the mobility of ions can be determined from the conductance behavior of the two systems. The values of specific conductance (k) of different concentrations of L-methionine from (0.0010, 0.0025, 0.0040, 0.0055, 0.0070, 0.0085) molalities in aqueous BTMAC and BTEAC solutions in the concentration range from 0.001 to 0.005 molality at different temperatures are provided in Tables S9–S11. Consequently, results from the conductance experiments listed in Table 10, along with Figures 5 and 6, showed that molar conductivity (Λ) values increase with an increase in temperature, and the continuous addition of L-Met into the IL solution causes a continuous decrease in molal conductivity of the solution.

Similar types of observations were found from the interaction between the amino acid (L-L-cysteine or glycine) and IL (BTEAC) solution.⁵³ However, it has been observed from the molar conductance (Λ) values listed in Table 10 that the molar conductance values are lesser in L-methionine in the aqueous solution of BTEAC than L-methionine in aqueous BTMAC solutions under all conditions. Similar types of outcomes have been observed for other amino acids from the literature.²⁷ However, under all conditions, the (L-Met + Aq. BTEAC) system has smaller values compared with other systems studied here. The use of specific conductance, $\kappa/(mS/cm)$, values obtained from the studied system at various temperatures can be transferred into molar conductance, $\Lambda/(mS \cdot cm^2 \cdot mol^{-1})$, by the following equation⁵⁷

$$\Lambda = (1000 \kappa)/c \quad (17)$$

Extrapolation of $\sqrt{c} = 0$ was carried out for the linear conductivity curves between Λ vs \sqrt{c} , for calculating the limiting molar conductance (Λ°) of AA (amino acid) in solutions of IL. ILs have $C_6H_5CH_2N^+(CH_3)_3$, $C_6H_5CH_2N^+(CH_3CH_2)_3$, and chloride anion in their structures. Thus, the terminal $-COO^-$ functional group of L-methionine interacts with the N^+ center of $C_6H_5CH_2N^+(CH_3)_3$ and $C_6H_5CH_2N^+(CH_3CH_2)_3$ ring through an ion–dipole interaction (Scheme 1).

The +I effect of three methyl (CH_3) groups and three ethyl (CH_2CH_3) groups of ILs is also considered another deciding factor in the amino acid (AA). Thus, BTEAC has more +I effect than BTMAC. Due to more lone-pair availability of oxygen atoms on the ($-COOH$) group, the molecular interaction is more prominent in the studied (L-Met + Aq. BTEAC) system than in the other studied systems. Higher conductance in the L-Met BTMAC solution than in the L-Met BTEAC solution is due to the presence of more available free ions. The mobility of the ionic species in a solution plays a very important role in molar conductance, in spite of the increasing number of ionic species with added L-methionine solution in time, as a result the molal conductivity is decreasing.⁵⁷ It may be caused by the increasing solute–solvent interaction between

Table 11. Values of Surface Tension (σ) of the (L-Methionine + Aq. BTMAC) System and the (L-Methionine + Aq. BTEAC) System in Aqueous ILs at Various Concentrations at Room Temperature and Pressure at 1.013 Bar^a

amino acid concentrations (mol·kg ⁻¹)	data of surface tension of the (L-methionine + Aq. BTMAC) system σ (mN m ⁻¹)	data of surface tension of the (L-methionine + Aq. BTEAC) system σ (mN m ⁻¹)
		0.001 <i>m</i> IL
0.0010	59.3	59.8
0.0025	60.3	60.6
0.0040	61.9	61.3
0.0055	62.3	62.5
0.0070	62.6	63.4
0.0085	64.3	64.8
		0.003 <i>m</i> IL
0.0010	56.3	56.6
0.0025	57.8	60.2
0.0040	60.1	64.2
0.0055	60.3	66.4
0.0070	62.3	67.8
0.0085	63.2	69.2
		0.005 <i>m</i> IL
0.0010	58.0	58.9
0.0025	58.6	61.2
0.0040	59.0	63.5
0.0055	59.6	64.9
0.0070	60.1	66.1
0.0085	60.8	69.5

^aStandard uncertainties in u (σ) = ± 0.1 (mN m⁻¹) (confidence level of the measurements is 0.68). # Considering the purity of mass of the chemicals, the combined standard uncertainty in molality is expected to be ± 0.0147 mol·kg⁻¹. * The mixture of water and IL is considered the solvent (kg⁻¹), and this has been expressed as molality.

IL and amino acids, which is governed by dipole–dipole, ion–dipole, and hydrophobic–hydrophobic interactions in solution mixtures between the solute and solvent molecules. Due to the solute–solvent interaction, development of molecular association between a solute and solvent increases on increasing the strength of the solute–solvent interaction, resulting in loss of their self-governing movement and decreasing the mobility of the ionic species in a solution. In this way, the conductometric measurement also gives similar results to those obtained from the volumetric, viscometric, and refractometric measurements.

3.5. Surface Tension. Surface tension (σ) is a very significant characteristic of liquids. Analysis of surface tension is of great significance in many scientific and technological fields. As an important parameter, surface tension is the most unique available experimental parameter that describes the thermodynamic features and provides information about the internal structure of the studied liquid systems. Notable indication about the interactions between solutes and solvents in the ternary systems (IL+ amino acid + H₂O) can be obtained from surface tension (σ) measurements. Solute amino acid molecules have surface-active property as described in an earlier study.⁵⁸ Here, the studied solvent systems contain a hydrophilic head group of two ILs (BTEAC and BTMAC) with a positive charge and the hydrophobic tail group acts as a prominent surface-active agent. Thus, this study is of immense interest in understanding the surface phenomena. The exploratory data for the measurements of surface tension (σ) in an aqueous medium of L-methionine amino acid in the presence of different molalities of aqueous ILs are listed in Table 11 at 298.15 K.

It was found from Figures S5 and S6 that the surface tension values vary linearly with an increase in concentration of amino acids. This type of linear increase of surface tension data

reveals that with an increase in the concentration of amino acid molecules, they interact to a greater extent with the IL, and as a result, the amino acids moved toward the bulk of the solutions from the surface. This is definitely due to solvophobic interactions among ionic liquids (ILs); as a result, the molecules of ionic liquids (ILs) can easily aggregate in water and aggregation is the highest in the case of 0.005*m* studied IL, and as a consequence, the surface tension is the minimum at this molality of IL.⁵⁹ Furthermore, the surface tension values of the (L-Met + Aq. BTEAC) system are higher compared to those of the (L-Met + Aq. BTMAC) system.

The sign and the extent of magnitude of slopes ($\partial\sigma/\partial m$) of surface tension obtained from Figures S5 and S6 cited above characterize the hydrophobic and hydrophilic nature of the solute with respect to the different molalities. This type of interaction associated with the solute molecules mainly prevails in the surface region.^{60,61} Using the surface tension values listed in Table 12, the limiting slopes obtained from the plots were considered very crucial factors when determining the very dilute region and area.

The limiting slopes ($\partial\sigma/\partial m$) for both systems are positive, as observed from Table 12, but higher values of the limiting slope were found in the case of the (L-Met + Aq. BTEAC) system. Similar trends of results were observed in the literature.⁵³ The positive values of both systems indicate a very typical electrolyte and polar hydrophilic nature of the compounds,⁶² and this was achieved by the favorable interaction between the zwitterion group (NH₃⁺ and COO⁻) of the amino acid (L-methionine) and the polar part (N⁺ and Cl⁻) of the ionic liquid (BTEAC and BTMAC). Due to the presence of the hydrophobic part (–CH₃ and –CH₂–CH₂–) of L-methionine, this can be readily absorbed at the interface between liquid and air.

Table 12. Data of Limiting Slopes ($\partial\sigma/\partial m$) of the Surface Tension of (L-Met + Aq. BTMAC) and (L-Met + Aq. BTEAC) Systems in Aqueous ILs at Various Concentrations^a

aqueous IL mixture	$(\partial\sigma/\partial m)/\text{mN m}^{-1}\cdot\text{kg}\cdot\text{mol}^{-1}$	
	L-Methionine + Aq. BTMAC	L-Methionine + Aq. BTEAC
0.001	61.9	68.8
0.003	76.6	106.7
0.005	88.6	117.1

^aStandard uncertainties in $u(\sigma) = \pm 0.1$ (mN m⁻¹) (confidence level of the measurements is 0.68). # Considering the purity of mass of the chemicals, the combined standard uncertainty in molality is expected to be ± 0.0147 mol·kg⁻¹. * The mixture of water and IL is considered the solvent (kg⁻¹), and this has been expressed as molality.

The cosphere overlap model⁵⁵ can explain the above results. In the ternary phase (IL + amino acid + H₂O), four types of molecular interactions exist for explaining the above facts according to the concept of the cosphere overlap model. (i) Hydrophilic–ionic interactions, i.e., interactions exist between the hydrophilic part of AA (NH₃⁺, COO⁻) and the ionic part of ILs; (ii) hydrophobic–ionic interactions, i.e., interactions between the hydrophobic part of L-methionine amino acid and ions of ILs; (iii) hydrophobic–hydrophobic interactions, i.e., interactions between the hydrophobic part of AA and the alkyl (CH₂–CH₂– and –CH₃) parts of ILs; and (iv) hydrophilic–hydrophobic interactions, i.e., interactions between the hydrophilic parts of AA and the hydrophobic parts of ILs (BTMAC and BTEAC).^{63,64}

3.6. FTIR Analysis. Fourier transform infrared spectroscopy (FTIR) was used to investigate the formation of hydrogen bonds between the solute (benzyl trimethyl ammonium chloride or benzyl triethyl ammonium chloride) and solvent (aqueous L-methionine) molecules. Every pure substance has its own characteristic infrared spectrum different from that of other substances. The spectral picture thus helps in confirming and identifying the sample of pure variety.

The FTIR spectra of pure ILs and pure amino acid (Figure 7) show some common absorption peaks at frequencies such as 3431.6, 3403.5, and 3428.2 cm⁻¹ for aliphatic C–H groups

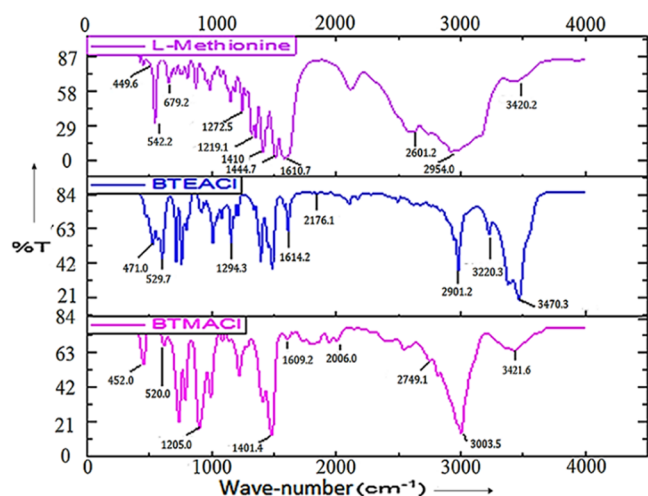


Figure 7. FTIR spectra of pure ILs (BTMAC and BTEAC) and AA (L-Met).

present in these molecules. Besides this, the existence of the H₂O molecule in a sample is identified by these specific absorption bands in this region along with additional peaks at 1609.2, 1614.6, and 1610.7 cm⁻¹ for BTMAC, BTEAC, and L-Met, respectively. The bands observed at 520, 452 cm⁻¹ for BTMAC, 529.7, 471.8 cm⁻¹ for BTEAC, and 543.2, 449.6 cm⁻¹ for L-Met confirm the presence of the H₂O molecule as lattice water with these molecules.⁶⁵

When L-Met and BTMAC are mixed in the ratios of 1:3, 2:2, and 3:1, the absorption peaks obtained for the mixtures are obtained in the FTIR spectra, as shown in Figure 8. When L-

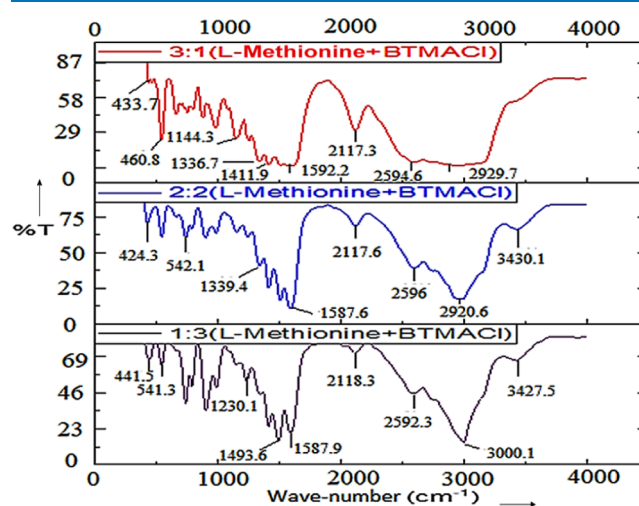


Figure 8. FTIR spectra of the L-Met + BTMAC mixture (AA/IL = 1:3, 2:2, 3:1).

Met and BTEAC are mixed in the ratios of 1:3, 2:2, and 3:1, the absorption peaks obtained for the mixtures are obtained in the FTIR spectra, as shown in Figure 9. The spectra show that the common bands for the amino acid and ILs are retained in the figures.

All fundamental vibrations that occur above 2500 cm⁻¹ nearly can be considered the stretching mode of hydrogen. The frequency and broadness of the band decrease for the hydrogen-bonding O–H system. The stretching mode of vibration of the N–H bond occurs in the 3300–3400 cm⁻¹ region. These bands often overlap the hydrogen-bonded O–H

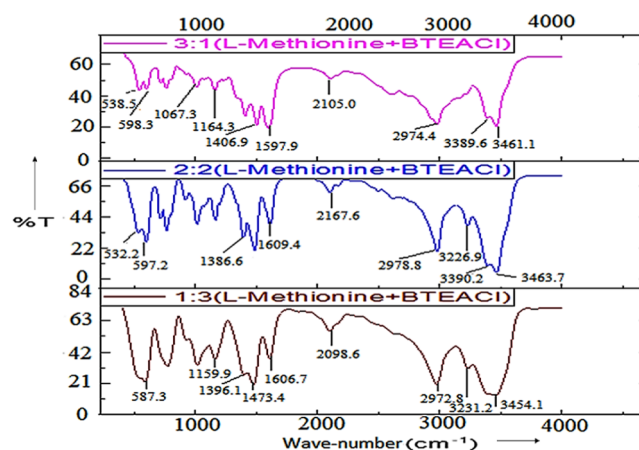


Figure 9. FTIR spectrum of the L-Met + BTEAC mixture (AA/IL = 1:3, 2:2, 3:1).

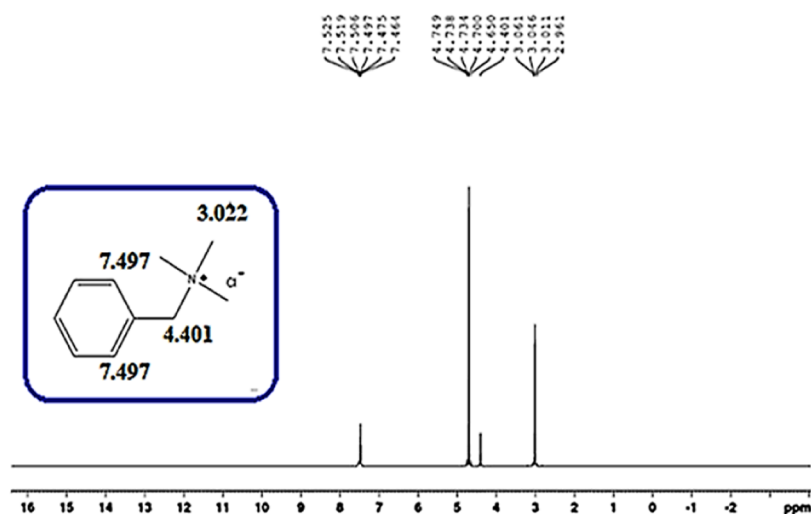


Figure 10. $^1\text{H-NMR}$ spectra of pure BTMAC in D_2O .

bands, but the peaks obtained from the N–H bands are normally sharper than those of the O–H bands. In ammonium and alkyl ammonium ions, frequencies occur in the region $2900\text{--}3200\text{ cm}^{-1}$ for the N–H stretching mode of vibrations. The C–H stretch occurs in the region $2850\text{--}3000\text{ cm}^{-1}$ for the aliphatic compound, L-Met, and in the region $3000\text{--}3100\text{ cm}^{-1}$ for the aromatic compounds, BTMAC and BTEAC. Absorptions corresponding to S–H occur at 2500 cm^{-1} . The stretching mode of vibrations for the double-bonded molecules and the bending mode of vibrations for the C–H, O–H, and N–H groups occur in the $2000\text{--}1600\text{ cm}^{-1}$ region.

The fingerprint region for the studied organic compounds here is observed below 1600 cm^{-1} . In this region, similar type of spectra is noticed for the substances, which shows that they are very much alike. The individual single bonds undergo coupling with each other, and their force constants and masses are similar. These are the groups of single bonds like C–O, C–C, and C–N, whose stretching vibrations often couple. Depending on the molecular skeleton of a given functional group in the cited region, the difference in frequency of absorption bands is observed for the functional group due to the involvement of a considerable number of oscillations of atoms of the skeleton of the molecule for each vibration.

The regular recurrence of some absorption bands when certain groups are present in the molecule points to the fact that these bands are characteristic of those groups. All compounds having a C–H bond exhibit bands in the region $3200\text{--}3500\text{ cm}^{-1}$. The exact position of the band is somewhat influenced by the rest of the molecule. In the ionic liquids and amino acid aqueous solution mixtures, the C–H band is observed around 3250 cm^{-1} , the N–H bonds have bands at $2900\text{--}3000\text{ cm}^{-1}$, and the O–H bands at $2700\text{--}2800\text{ cm}^{-1}$.

This is very useful as it confirms the presence of a group in a molecule. In a mixture, the positions and intensities of the bands for a particular substance are not affected by the presence of other components. Thus, in a mixture of closely related compounds, the identification as well as the quantitative estimation of a particular component can be spectroscopically ascertained. Broad peaks around 3427.5 cm^{-1} in the 1:3 L-Met and BTMAC aqueous mixture are observed, which show that both surface free hydroxyl groups and chemisorbed water are present in this system due to the overlapping of O–H and N–H stretching vibrations groups.

The peaks around 2929.7 cm^{-1} in the 3:1 L-Met and BTMAC solution and around 1386.6 cm^{-1} in the 2:2 L-Met and BTEAC solution correspond to the C–H symmetric stretch of the methylene groups ($-\text{CH}_2-$) and deformation vibration of the methyl groups ($-\text{CH}_3$). The peak is at 1252.7 cm^{-1} in the 3:1 L-Met and BTMAC solution for the C=O stretching vibration of carboxylate ($-\text{COO}^-$) groups. Due to the change in bond energy, shifts in wave numbers of the mentioned functional groups are also observed.⁶⁶

The peaks at 1609.4 and 1597.9 cm^{-1} in 2:2 and 3:1 L-Met and BTEAC solutions are indicative of an asymmetric $-\text{COO}^-$ stretching bond (carboxylate), and the peaks at 1413.1 and 1406.9 cm^{-1} in the 2:2 L-Met and BTMAC solution indicates a symmetric $-\text{COO}^-$ stretching bond.⁶⁷ In addition, there was a new peak at 3231.2 cm^{-1} in the 1:3 L-Met and BTEAC aqueous solution due to N–H stretching after absorption.⁶⁸

At $600\text{--}700\text{ cm}^{-1}$, absorption bands are visibly detected in 2:2 and 3:1 L-Met and BTMAC solutions due to OH out-of-plane bending. Therein, the unusual stretching mode of C–O and C–C bonds, rocking of CH_2 , and other skeletal modes not easily detected in other organic molecules give their unique IR signatures. The peaks at 1272.5 and 1319.1 cm^{-1} in L-Met are related to the stretching, bending, and rocking of $-\text{CH}_2$ groups. Around 1600 cm^{-1} as expected, the most prominent features originate from the functional group ($-\text{COO}-$) owing to the IR absorption in the L-Met and BTEAC solutions.^{69–71}

Thus, from the above observations and nature of the spectra, it may be concluded that the aqueous mixture of L-methionine and BTEAC when mixed in the ratio 3:1 (Figure 9) indicates the highest interactions and that the 1:3 ratio of L-methionine and BTMAC exhibits the lowest interactions (Figure 8). Thus, FTIR spectroscopy was found to be one of the utmost suitable methods for studying the molecular interactions in solutions.⁷²

3.7. $^1\text{H-NMR}$ Studies. We thus see that nuclear magnetic resonance studies^{73–75} reveal the presence of particular functional groups, the relative number of nuclei present in the group, and the relative positions of these groups from the multiplicities of the lines. Hence, NMR provides the means for investigating in depth the details of the internal structure of molecules not available through other methods. It is a very useful technique for chemists to derive the resonance energy, which totally depends on the nature of the electronic environment about the nucleus.

The chemical shift, δ , provides the difference in the shielding constants of the sample and the reference. In a solvent, both shielding of electrons and the volume diamagnetic susceptibility of the solvent influence the chemical shift of a solute molecule. The diamagnetic contributions to the shielding of the solute would depend on the average number of solute as well as solvent molecules; therefore, the chemical shift will be concentration-dependent. There are more intermolecular interactions associated with concentrated solutions than with dilute solutions. A lower field of chemical shift is observed due to the lowest screening of the proton by this type of molecular interaction.⁷⁶

The presence of a static part of a nucleus causes a very small change in the effective magnetic field of another nucleus. By changing the effective magnetic field in the presence of a second nucleus, the variation of the angle, distance, and magnitude of the field can be changed. Therefore, this type of effect sharply decreases with distance and only very close molecules effectively change the magnitude of the field. Due to the random arrangements of neighboring molecules in this environment, the nuclei of this molecule undergo precisely the NMR transition. Thus,^{13,77} $^1\text{H-NMR}$ is an effective device to investigate the variations of the electronic environment near the various protons of IL in the presence of amino acids. The chemical shift value (δ) of various protons of AA and the IL studied depends on the electron density present in their surrounding area.

Here, $^1\text{H-NMR}$ spectroscopy of pure BTMAC, BTEAC, and L-Met and in the mixture of amino acid with ILs was performed. The values of chemical shift of different protons (δ_1 – δ_3) of BTMAC and (δ_1 – δ_4) BTEAC in the D_2O solvent are cited in Figure 10 and Figure 11, separately. The $^1\text{H-NMR}$

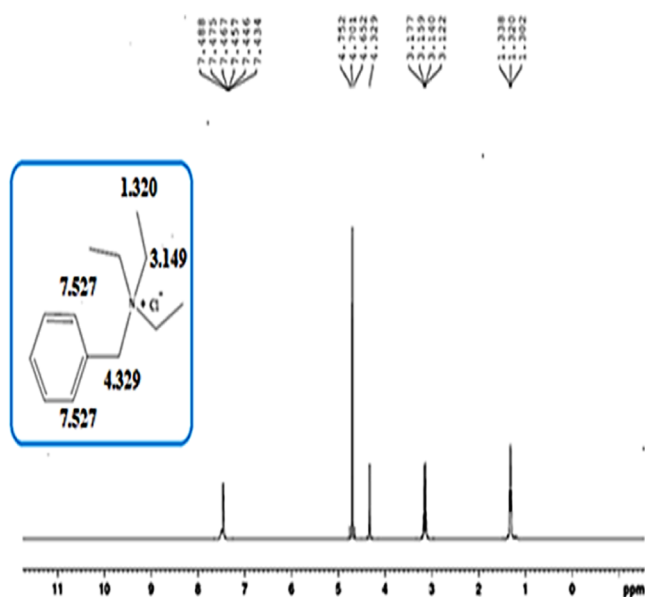


Figure 11. $^1\text{H-NMR}$ spectra of pure BTEAC in D_2O .

spectroscopy technique showed that there were three characteristic peaks of this $[\text{BTMA}]^+$ ion corresponding to the terminal $-\text{CH}_3$ (δ_1) protons of the alkyl chain at 3.022 ppm, benzyl- CH_2 (δ_2) protons at 4.401 ppm, and $-\text{C}_6\text{H}_5$ protons (δ_3) at 7.497 ppm. In addition, there were four characteristic peaks of the ion $[\text{BTEA}]^+$ corresponding to terminal- CH_3 (δ_1) protons at 1.320 ppm of the ethyl chain,

$-\text{CH}_2$ (δ_2) protons at 3.149 ppm of the ethyl chain, benzyl- CH_2 (δ_3) protons at 4.329 ppm, and $-\text{C}_6\text{H}_5$ protons (δ_4) at 7.527 ppm. The (δ) values of various protons of L-Met in the D_2O solvent are shown in Figure 12. It was also observed from the $^1\text{H-NMR}$ spectrum of L-methionine that in this spectrum four distinguishing peaks were noticed for the terminal protons of the $-\text{CH}_3$ (δ_1) group at 2.054 ppm, protons of the $-\text{CH}_2$ (δ_2) group at 2.552 ppm, protons of the $-\text{CH}_2$ (δ_3) group at 2.096 ppm, and also the protons of methane ($-\text{CH}$) (δ_4) directly attached to $-\text{NH}_2$ group at 3.753 ppm.

The moieties present in any compound around the close vicinity of protons are the factors that determine the chemical shift (δ) values of protons. In this connection, Figures 13 and B14 show the NMR spectra of two systems, (BTMAC + L-methionine) and (BTEAC + L-methionine), in which chemical changes of protons in the ratio 4:1 in the D_2O solvent were observed. The shielding and deshielding effects of groups of any compound depend on the chemical shift (δ) values to upfield (lower frequency) or downfield (higher frequency). Due to the interactions associated with the ionic liquid and the amino acid, the chemical shift values of protons of BTMAC were observed to move toward the lower-frequency region, which is called the upfield shift of the protons, and this was observed from our present $^1\text{H-NMR}$ study. In this connection, upfield chemical shift values were also found in L-methionine amino acid. The chemical shift values of protons of ionic liquid (BTEAC and BTMAC) and amino acid (L-methionine) move upfield due to an increase in the density of the electron around this, which may be responsible for the intermolecular interactions prevailing among the ionic liquids and amino acid.

Figures 13 and B14 display the $^1\text{H-NMR}$ spectra for the determination of chemical shift changes of each proton of the mixture of amino acid with ionic liquid in the ratio of 4:1 by comparing with their corresponding pure BTMAC, BTEAC, and pure amino acid. The $^1\text{H-NMR}$ spectra showed that the chemical shift (δ_1) at the terminal $-\text{CH}_3$ protons shifted from 3.022 to 3.010 ppm, the chemical shift (δ_2) of benzyl- CH_2 protons shifted from 4.401 to 4.405 ppm, and the phenyl ring (δ_3) protons shifted from 7.497 to 7.494 ppm of the BTMAC, and it has also been found from the BTEAC ionic liquid that the chemical shift (δ_1) at terminal $-\text{CH}_3$ protons shifted from 1.320 to 1.214 ppm, the chemical shift (δ_2) of $-\text{CH}_2$ (δ_2) protons shifted from 3.149 to 3.130 ppm, and similarly the chemical shift (δ_3) of benzyl- CH_2 protons shifted from 4.329 to 4.310 ppm and the phenyl ring (δ_4) of protons shifted from 7.527 to 7.464 ppm. However, it has been observed very carefully that the magnitude of an upfield shift of BTEAC is much higher compared with BTMAC in the presence of L-Me, as shown in the cited figure in Figures 13 and B14. The chemical shifts (δ) of protons at the terminal position- CH_3 (δ_1) of protons at the terminal position- CH_3 (δ_1) of BTMAC shifted from 3.022 to 3.010 ppm, of protons of benzyl- CH_2 (δ_2) of BTMAC shifted from 4.401 to 4.405 ppm, of protons of BTEAC at the terminal- CH_3 (δ_1) shifted from 1.320 to 1.214 ppm, of protons of the ethyl chain- CH_2 (δ_2) shifted from 3.149 to 3.130 ppm, and also of protons of the benzyl- CH_2 (δ_3) shifted from 4.329 to 4.310 ppm, giving the smallest chemical shift changes; very significant chemical shift changes were observed (from 2.054 to 1.993 ppm) for the terminal $-\text{CH}_2$ (δ_1) protons attached with the S atom and $-\text{CH}_2$ (δ_2) protons connected with the S atom shifted from 2.552 to 2.548 ppm, $-\text{CH}_2$ (δ_3) protons moved from 2.096 to 1.301 ppm and $-\text{CH}$ (δ_3) protons directly attached with $-\text{NH}_2$ group shifted from 3.753 to 3.759 ppm of L-Met in the case of the (L-Met +

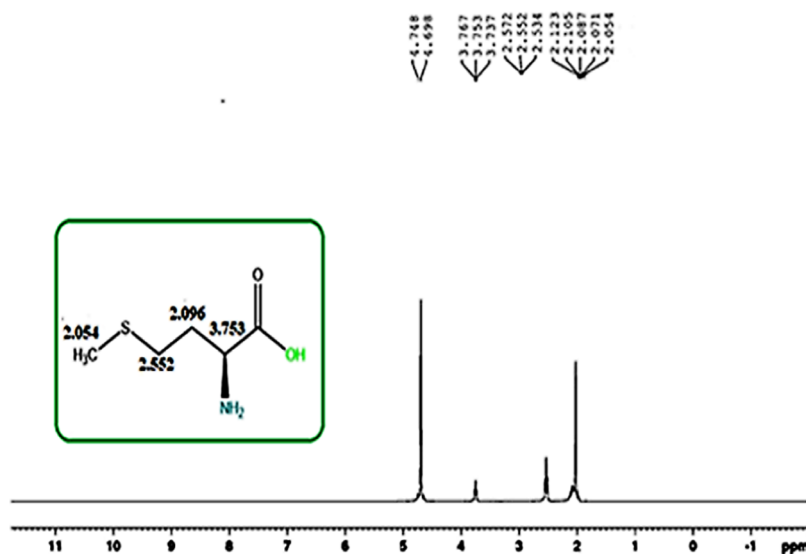


Figure 12. ^1H -NMR spectra of pure L-methionine in D_2O .

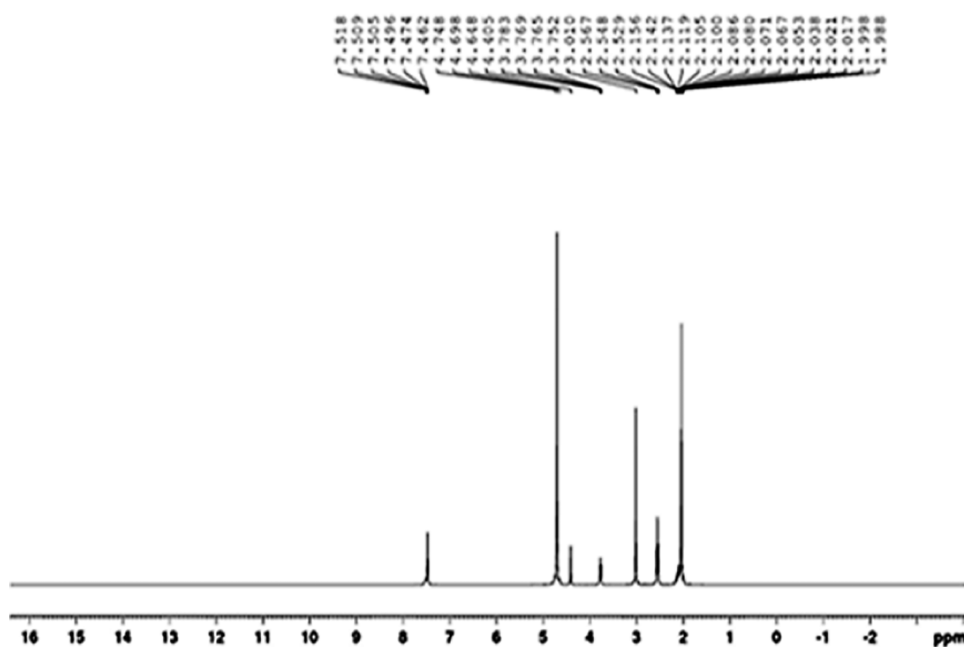


Figure 13. ^1H -NMR spectrum of L-Met + BTMAC (AA/IL = 4:1) in D_2O .

BTMAC) system; also, a significant chemical change is observed for protons closer to $\text{S}-\text{CH}_3$ ($\delta 1$), which shifted from 2.054 to 2.062 ppm, $-\text{CH}_2$ ($\delta 2$) protons moved from 2.552 to 2.541 ppm, $-\text{CH}_2$ ($\delta 3$) protons moved from 2.096 to 1.336 ppm, and $-\text{CH}_2$ ($\delta 4$) directly attached to the group of $-\text{NH}_2$ shifted from 3.753 to 3.766 ppm. However, if we compare the change of chemical shift between the two systems (L-Met + BTMAC) and (L-Met + BTEAC), a higher chemical shift of protons was found in the case of the L-Met + BTEAC system.

The above results give us an idea about the nature of interactions connected with the studied system, and it was found that the hydrophobic interactions mainly occur between the hydrophobic part of alkyl chains and the phenyl group of ILs, BTMAC and BTEAC, and the hydrophobic portion of the $-\text{CH}_3$ group attached to the sulfur atom, the $-\text{CH}_2$ group attached to the sulfur atom, one $-\text{CH}_2$ group and one $-\text{CH}$

group of L-Met attached to the $-\text{NH}_2$ group.^{78,79} It has also been noticed that the hydrophobic interaction in the (BTEAC + L-Met) system is more since the upfield shifts are more in the case of the mentioned different portions of the chemical shift values of $-\text{CH}_3$ ($\delta 1$), $-\text{CH}_2$ ($\delta 2$), phenyl ring ($\delta 3$), phenyl ring ($\delta 4$), protons of BTEAC and $-\text{CH}_3$ ($\delta 1$), $-\text{CH}_2$ ($\delta 2$) attached to the S atom, and $-\text{CH}$ ($\delta 3$) protons of L-Met compared to the (BTMAC + L-Met) system.

The nature of the spectra, number, intensity, and broadness of the peaks obtained by proton NMR spectroscopy of the systems mixed in the ratio of (4:1) (AA/IL) shows that the aqueous mixture of L-methionine and BTEAC (Figure 14) exhibits more interactions compared to the aqueous mixture of L-methionine and BTMAC (Figure 13).

Thus, the NMR data give us a confirmation about the probable contributing aspects such as ion-dipole and ion-ion interactions associated with amino acid (AA) and ILs and the

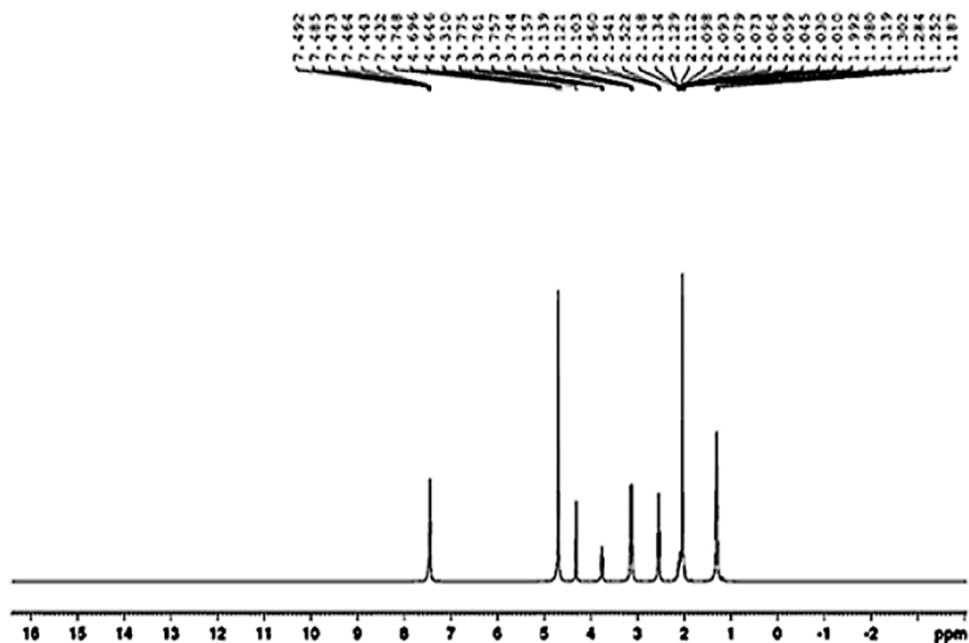
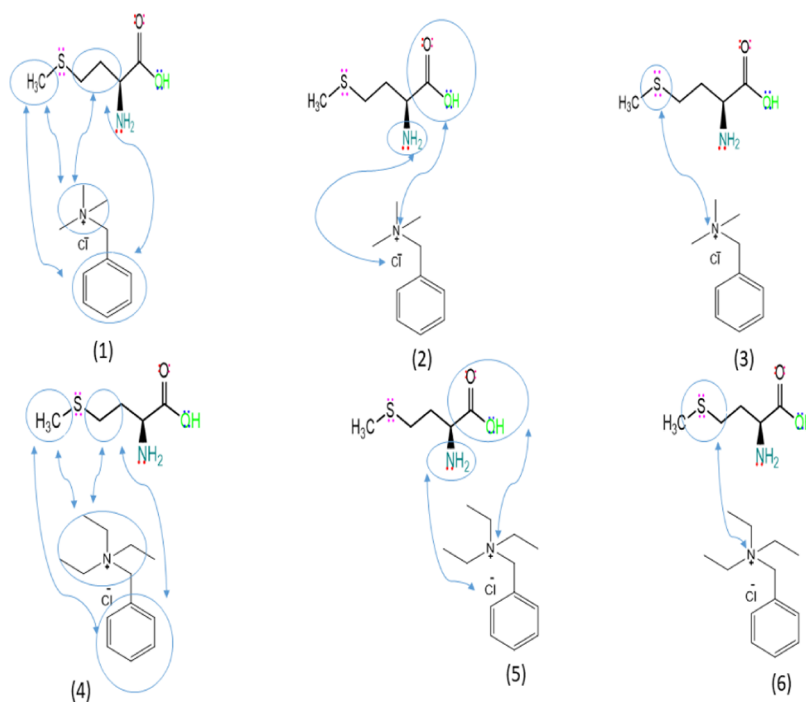


Figure 14. $^1\text{H-NMR}$ spectrum of *L*-Met + BTEAC (AA/IL = 4:1) in D_2O .

Scheme 2. Representations of Different Molecular Interactions Schematically Associate with Two Ionic Liquids with One Amino Acid: (1, 4) Hydrophobic–Hydrophobic Interactions; (2, 5) Ion–Ion Interactions; (3, 6) Ion–Dipole Interactions



hydrophobic interactions incorporated within the system.^{42,48} The possible types of interactions occurring in the studied systems (*L*-Met + Aq. BTEAC) and (*L*-Met + Aq. BTMAC) are presented in Scheme 2. The conclusion from NMR measurements gives similar types of results as obtained by FTIR studies between ILS and the AA studied here.

3.8. UV–Visible Spectra Measurement. In this study, the binding nature and stability of the molecular association were carried out between AA (*L*-Met) and ionic ILs (BTMAC and BTEAC). The association constant or stability constant (K_a) for the molecular association exhibited in the studied

system was measured with the help of the UV–vis spectroscopic technique.⁸⁰ The data obtained in the solution mixture from the above-mentioned technique helps determine the stability constant or the association constant. The absorption peaks of two ionic liquids in the aqueous solution by changing the concentration of amino acid (*L*-methionine) are shown in the reported Figures 15 and C16. The absorbance (ΔA) changes of BTMAC and BTEAC at $\lambda_{\text{max}} = 208 \text{ nm}$ (Figures 15 and C16, respectively) on changing the concentration of *L*-methionine solutions from a lower to a higher value by the UV-spectroscopic technique were

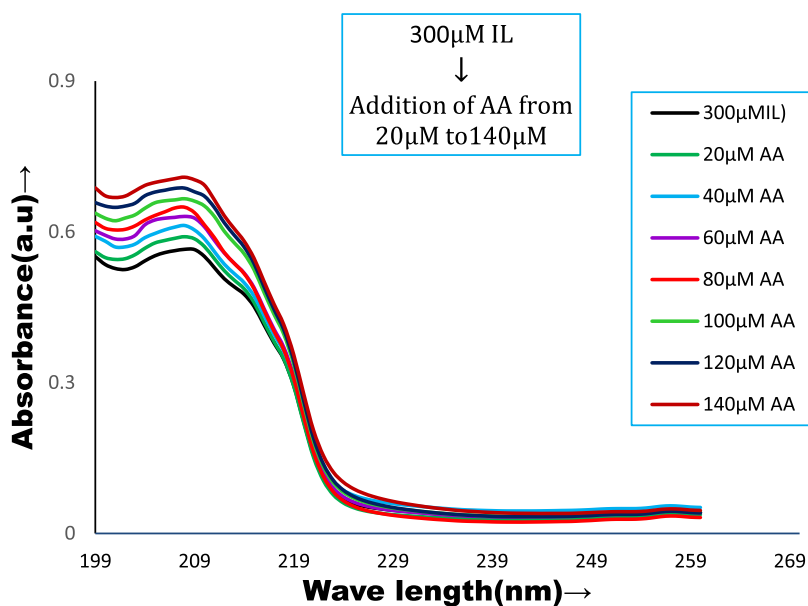


Figure 15. UV-vis spectra of the (BTMAC + L-Met) system.

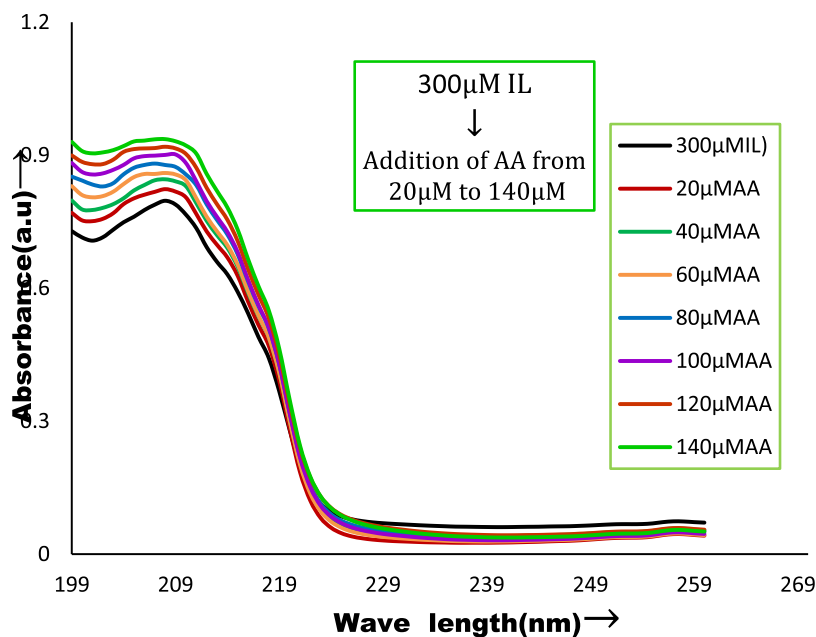


Figure 16. UV-vis spectra of the (BTEAC + L-Met) system.

considered for the determination of the association constant (K_a) at 298.15 K.

The interaction phenomenon between the ILs with one amino acid was calculated using one of the very commonly used and popular techniques (the Benesi–Hildebrand method) to derive the association constant (K_a). The double reciprocal plots ($1/\Delta A$ vs $1/[AA]$) for the studied systems were obtained from the Benesi–Hildebrand method using the following equation;²² the plots were found to be linear in nature, and all systems showed a good correlation ($R^2 > 0.900$) (Figures 17 and C18) that generally predicts the interactions (1:1) between the solute and solvent in solution.⁶¹

$$1/\Delta A = 1/\Delta\epsilon[IL] \cdot 1/[AA] + 1/\Delta\epsilon[IL] \quad (18)$$

where ΔA gives the changes in absorbance of ILs in the absence or presence of AA. [IL] indicates the concentration of

BTMAC and BTEAC. [AA] represents the concentration of L-methionine. The values of the association constant of the systems (BTMAC + L-Met) and (BTEAC + L-Met) were obtained as 2751 and 3850 M^{-1} from the slope/intercept of the plots using the Benesi–Hildebrand equation, and the results of the K_a value are listed in Tables 13 and 14.⁸⁰

For the molecular assembly, the change in free energy taking place between the amino acid and an ionic liquid can be achieved by the following association constant-free energy relationship

$$\Delta G = -RT \ln K_a \quad (19)$$

where ΔG denotes the change in free energy ($\text{kJ}\cdot\text{mol}^{-1}$), K_a denotes the association constant, R refers to the universal gas constant, and T is the temperature in Kelvin. Here, the values of ΔG for the studied system are given in Tables 13 and 14,

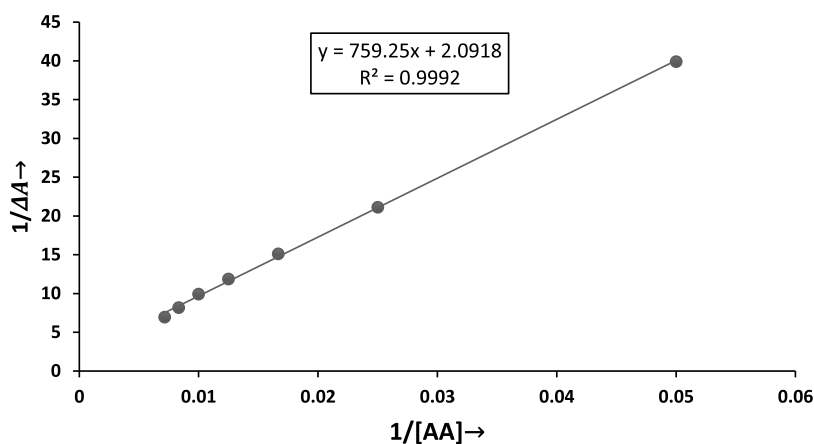


Figure 17. Benesi double reciprocal plot of the BTMAC + L-Met system.

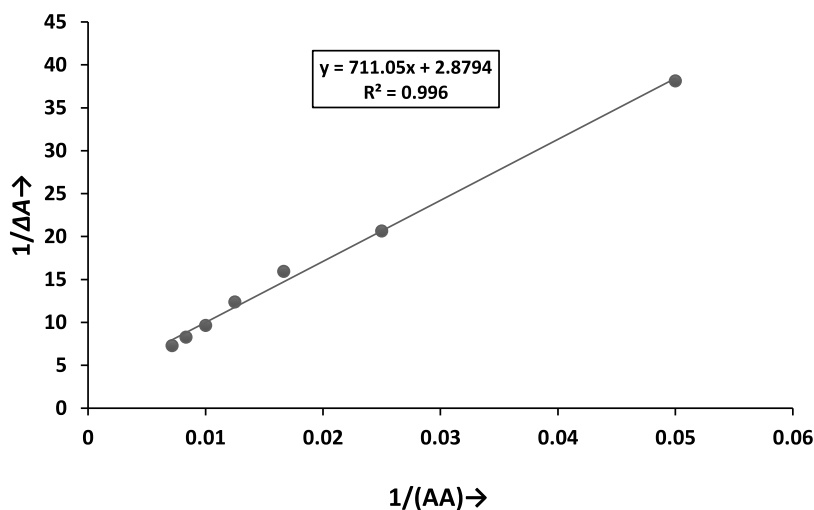


Figure 18. Benesi double reciprocal plot of the BTEAC + L-Met system.

Table 13. UV–Vis Spectroscopic Data for the Benesi–Hildebrand Double Reciprocal Plot of the BTMAC + L-Met System at 298.15 K^a

BTMAC + L-Met												
temp/K	IL/ μM	[AA]/ μM	A_0	A	ΔA	$1/[\text{AA}]/\text{M}^{-1}$	$1/\Delta A$	intercept	slope	$K_a/\text{M}^{-1} \times 10^{-3}$	$\Delta G/\text{kJ mol}^{-1}$	
300	20	0.56530	0.59036	0.02505	0.0500	39.1117	2.0918	759.25	2.75	-19.6		
	40	0.56530	0.61686	0.04736	0.0250	21.1107						
298.15	300	60	0.56530	0.63080	0.06617	0.0166	15.1107					
	300	80	0.56530	0.64903	0.08427	0.0125	11.8657					
	300	100	0.56530	0.66593	0.10090	0.0100	9.9108					
	300	120	0.56530	0.68707	0.12203	0.0088	8.1948					
	300	140	0.56530	0.70875	0.14375	0.0062	6.9589					

^aStandard uncertainties in temperature (T) = ± 0.01 K.

respectively, and the values of the negative sign of the Gibbs free energy of the systems (L-Met + BTMAC) and (L-Met + BTEAC) are -19.6 and -20.6 $\text{kJ}\cdot\text{mol}^{-1}$, respectively, which indicates the feasibility of the interactions between the AA and ILs. It was found from the listed table that the negative sign of ΔG and the positive value of K_a are more in the case of the (L-Met + BTEAC) system. Therefore, the molecular adduct formation between L-methionine and the ionic liquid (BTEAC) is more facile than that of the other studied systems.

3.9. Theoretical Study of Solute–Solvent (Amino Acid and IL) Interaction. Optimized geometries of L-Met-

BTMAC and L-Met-BTEAC composites are shown in Figure 19a,b. In both composites, a strong dipole–dipole interaction within the range of 2.28–3.34 Å exists between L-Met and the ionic liquid. The L-Met-BTMAC composite experiences a higher adsorption energy ($E_{\text{ads}} = -13.61$ $\text{kJ}\cdot\text{mol}^{-1}$) than the corresponding L-Met-BTEAC composite ($E_{\text{ads}} = -7.39$ $\text{kJ}\cdot\text{mol}^{-1}$). These data clearly indicate that the dipole–dipole interaction is prominent in both composite systems. This strong interaction is attributed to the presence of strong dipole–dipole interactions between the positive pole of ILs (hydrogens of the CH_2 group of methyl and ethyl groups) and

Table 14. UV–Vis Spectroscopic Data for the Benesi–Hildebrand Double Reciprocal Plot of the BTEAC + L-Met System at 298.15 K^a

BTEAC + L-Met											
temp/K	IL/ μ M	[AA]/ μ M	A_0	A	ΔA	$1/[AA]/M^{-1}$	$1/\Delta A$	intercept	slope	$K_a/M^{-1} \times 10^{-3}$	$\Delta G/kJ mol^{-1}$
300	20	20	0.79716	0.82339	0.02623	0.0500	38.1242	2.8794	711.05	3.85	-20.4
	40	40	0.79716	0.84560	0.04844	0.0250	20.6406				
298.15	300	60	0.79716	0.85986	0.06270	0.0166	15.9489				
	300	80	0.79716	0.87791	0.08070	0.0125	12.3915				
	300	100	0.79716	0.90063	0.10345	0.0100	9.6602				
	300	120	0.79716	0.91899	0.12093	0.0088	8.2695				
	300	140	0.79716	0.93426	0.13717	0.0062	7.2932				

^aStandard uncertainties in temperature (T) = ± 0.01 K.

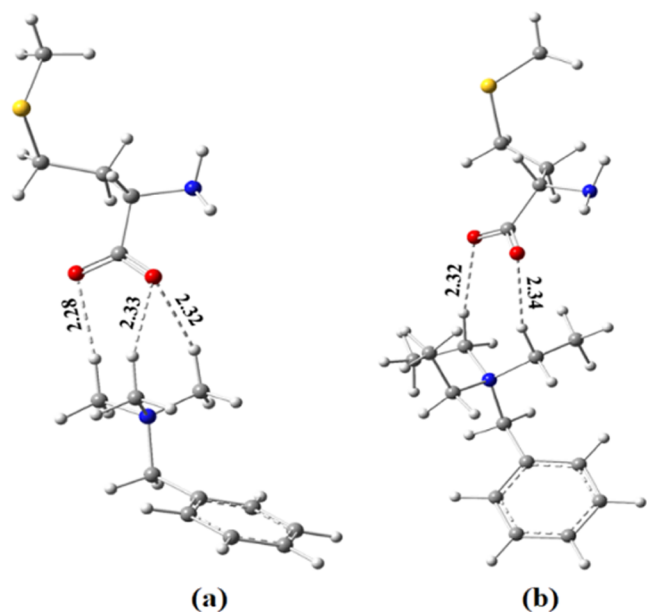


Figure 19. Optimized geometries of the (a) L-Met-BTMAC and (b) L-Met-BTEAC systems in an aqueous solution.

the negative pole of the amino acid (oxygen of the carboxylate group) indicated by the broken line (-----) in Figure 19a,b.

This observation is consistent with the experimental NMR shifting and is concordant with a previous study.⁷⁵ To provide more insights into the hydrophobic and electrostatic interactions between L-Met and ionic liquid, we have plotted molecular electrostatic maps (ESPs), as illustrated in Figure 20. From the ESP maps, it is clear that the interaction is purely electrostatic (red region) and originates from the interactions between the carboxylic groups (negative pole) and the hydrogens of the methyl group (positive pole) connected with the nitrogen (N) atom of the ionic liquids. The red region of ESP maps for L-methionine-BTEAC is more prominent than that of L-methionine-BTMAC, indicating the presence of profound electrostatic interaction in the former than in the latter.

To understand the weak interactions like van der Waals, H-bonding, and steric interaction present in amino acid-IL complexes, we have analyzed the RDG plots^{53,82} as shown in Figure 21. The existence of dipole–dipole interactions in the composites has also been confirmed by the scattered area of the negative region of the RDG plot (0.01–0.02 region) for both composite systems (Figure 21). Similar types of results

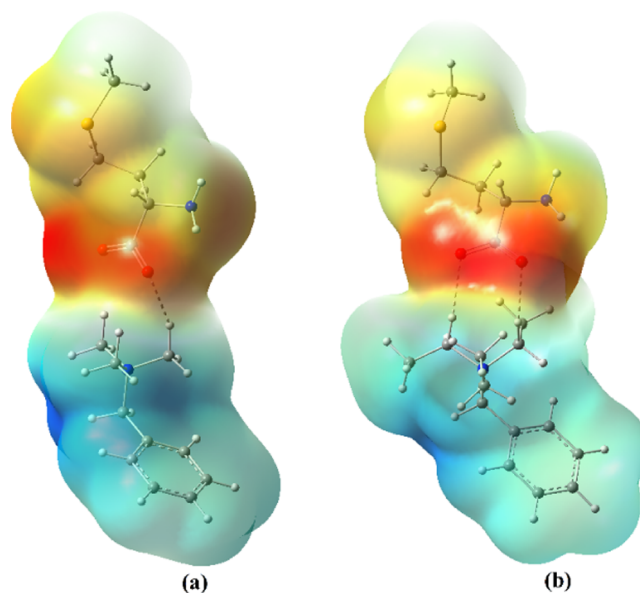


Figure 20. Electrostatic potential maps for (a) L-Met-BTMAC and (b) L-Met-BTEAC in an aqueous medium.

have been observed between the amino acid L-cysteine/glycine-BTEAC ionic liquid system in a previous study.⁵³

4. CONCLUSIONS

Experimental observations between one amino acid, L-methionine (L-Met), and two significant ionic liquids, benzyl trimethyl ammonium chloride (BTMAC) and benzyl triethyl ammonium chloride (BTEAC), in an aqueous medium at various temperatures with some parameters, such as density, viscosity, refractive index, conductance, and surface tension measurements, were supported by FTIR, ¹H-NMR, and UV–vis spectroscopies. This provided us with the information of strong solute–solvent interactions in (L-Met + Aq. BTMAC) and (L-Met + Aq. BTEAC) systems predominant over the solute–solute interactions. Amino acids have B -coefficient values that increase with temperature and positive values of dB/dT , indicating that they function as structure-disruptors, which is further verified by Hepler's constant values. Moreover, at 308.15 K, the interactions were found to be the highest for L-Met in 0.005*m* of aqueous IL (BTEAC) and the lowest at 298.15 K of L-Met in 0.001*m* of aqueous IL (BTMAC) for all parameters. The structure-breaking property was the strongest for the L-Met solution in 0.005*m* aqueous BTEAC (IL) [$(\delta\Phi_E^0/\delta T)_P = -0.0736 \times 10^{-6} m^3 \cdot mol^{-1} \cdot K^{-2}$], with the highest packing or caging effect. The solute–solvent

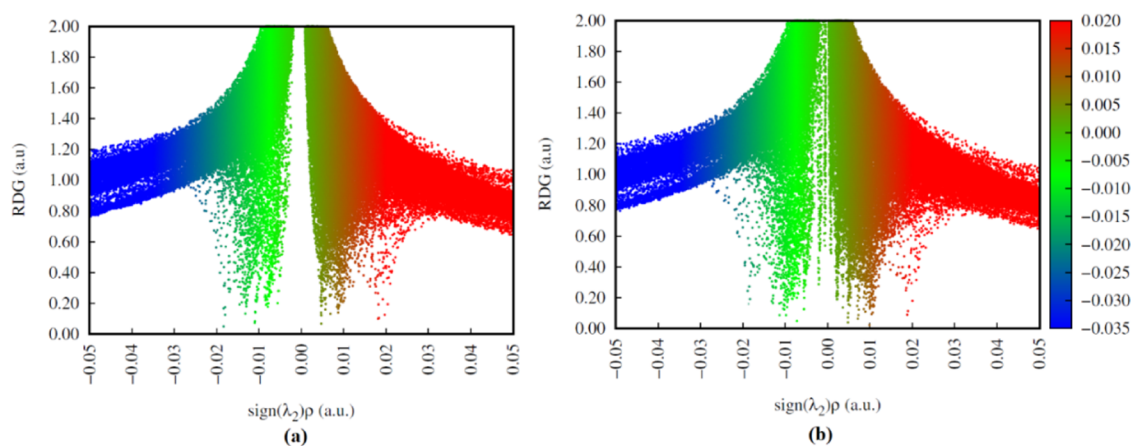


Figure 21. Reduced density gradient of (RDG) for (a) L-Met-BTMAC and (b) L-Met-BTEAC composites.

interactions in the transition state, resulting by the breaking and altering of intermolecular force, have been explained by the free energy of activation of viscous flow prevalent in the structure of the solvent medium. The greater values of $\Delta\mu_2^{\text{off}}$ for the L-Met + Aq. BTEAC system than for L-Met + Aq. BTMAC show the more effective structure-making ability of L-methionine in an aqueous BTEAC ionic liquid solution. Due to the larger alkyl group in BTEAC, which has a greater +I effect compared with BTMAC, the interaction is more dominant in the (L-Met + BTEAC) system than in the other system, which is concordant with our theoretical calculations. The degree of interaction between amino acid (L-methionine) and ionic liquids (BTMAC and BTEAC) gives us its usability in the field of pharmaceutical chemistry and cosmetology.

■ ASSOCIATED CONTENT

SI Supporting Information

The Supporting Information is available free of charge at <https://pubs.acs.org/doi/10.1021/acsomega.2c08008>.

Description of table for density, viscosity, molar refraction, refractive index, specific conductance, apparent molar volume; description of figure for variation of apparent molar volume, variation of molar refraction, variation of surface tension plot, and $^1\text{H-NMR}$ spectrum of ILs in D_2O solvent at 298.15 K (PDF)

■ AUTHOR INFORMATION

Corresponding Author

Mahendra Nath Roy – Department of Chemistry, University of North Bengal, Darjeeling 734013 West Bengal, India; Alipurduar University, Alipurduar 736123 West Bengal, India; orcid.org/0000-0002-7380-5526; Phone: +91-353-2776381; Email: mahendraroy2002@yahoo.co.in, vcapduniversity@gmail.com; Fax: +91 353 2699001

Authors

Sukdev Majumder – Department of Chemistry, University of North Bengal, Darjeeling 734013 West Bengal, India
Anuradha Sinha – Department of Chemistry, Siliguri College, Siliguri, Darjeeling 734001 West Bengal, India
Debadrita Roy – Department of Chemistry, University of North Bengal, Darjeeling 734013 West Bengal, India
Biswajit Ghosh – Department of Chemistry, University of North Bengal, Darjeeling 734013 West Bengal, India

Narendra Nath Ghosh – Department of Chemistry, University of Gour Banga, Malda 732103, India

Tanusree Ray – Department of Chemistry, Siliguri College, Siliguri, Darjeeling 734001 West Bengal, India

Vikas Kumar Dakua – Alipurduar University, Alipurduar 736123 West Bengal, India

Anupam Datta – Alipurduar University, Alipurduar 736123 West Bengal, India

Indu Bhusan Sarkar – Alipurduar University, Alipurduar 736123 West Bengal, India

Subhankar Choudhury – Department of Chemistry, Malda College, Malda 732101, India

Ashim Roy – Alipurduar University, Alipurduar 736123 West Bengal, India

Nitish Roy – Department of Chemistry, University of North Bengal, Darjeeling 734013 West Bengal, India

Complete contact information is available at:

<https://pubs.acs.org/doi/10.1021/acsomega.2c08008>

Author Contributions

S.M.: Conceptualization of the work, investigation of data, resources, writing—review & editing, writing—original draft. A.S.: Writing—original draft. D.R.: Writing—original draft. T.R.: review & editing. N.N.G.: Investigation, review, writing—original draft. B.G.: Investigation and review original draft. V.K.D.: Investigation and review original draft. A.D.: Investigation and review original draft. I.B.S.: Investigation and review original draft. S.C.: Investigation and review original draft. A.R.: Investigation, writing—original draft. N.R.: Writing—review & editing. M.N.R.: Conceptualization and supervision.

Notes

The authors declare no competing financial interest.

The authors declare that they have no known competing financial interests or personal relationships that could have appeared to affect the work in this manuscript.

■ ACKNOWLEDGMENTS

Prof. M.N.R. is grateful to the University Grant Commission (UGC), New Delhi, Government of India, for being awarded a one-time grant under Basic Scientific Research through the grant-in-Aid No. F.4-10/2010 (BSR) considering his active service for extending of research for further work and UGC supported project (ref No. RP/S032/FCS/2011, New Delhi) for providing instrumental facilities.

REFERENCES

- (1) Raza, M. A.; Hallett, P. D.; Liu, X.; He, M.; Afzal, W. Surface tension of aqueous solutions of small-chain amino and organic acids. *J. Chem. Eng. Data* **2019**, *64*, 5049–5056.
- (2) Ali, A.; Sabir, S.; Nain, A. K.; Hyder, S.; Ahamad, S.; Tariq, M.; Patel, R. Interactions of phenylalanine, tyrosine and histidine in Aqueous caffeine solutions at different temperature. *J. Chin. Chem. Soc.* **2007**, *54*, 659–666.
- (3) Barman, S.; Saha, B.; Majumder, S.; Roy, K.; Ray, T.; Sarkar, L.; Sinha, A.; Roy, M. N. Solvation consequences of some noteworthy molecules in diverse liquid environments explored by physicochemical methodologies. *J. Chem. Biol. Phys. Sci.* **2022**; Vol. 12 4 DOI: 10.24214/jcbps.a.12.4.33763.
- (4) Singh, V.; Singh, D.; Gardas, R. L. Effect of DBU (1,8-Diazabicyclo[5.4.0]undec-7-ene) Based Protic Ionic Liquid on the Volumetric and Ultrasonic Properties of Ascorbic Acid in Aqueous Solution. *Ind. Eng. Chem. Res.* **2015**, *54*, 2237–2245.
- (5) Shekaari, H.; Jebali, F. Densities, viscosities, electrical conductances, and refractive indices of amino acid+ ionic liquid ([BMIm] Br)+ water mixtures at 298.15 K. *J. Chem. Eng. Data* **2010**, *55*, 2517–2523.
- (6) Zhao, H. Viscosity B-coefficients and standard partial molar volumes of amino acids, and their roles in interpreting the protein (enzyme) stabilization. *Biophys. Chem.* **2006**, *122*, 157–183.
- (7) Ali, A.; Shahjahan, A. Volumetric and viscometric behaviour of some amino acids and their group contributions in aqueous tetramethylammonium bromide at different temperatures. *Z. Phys. Chem.* **2008**, *222*, 1519–1532.
- (8) Sumathi, T.; Varalakshmi, M. Ultrasonic velocity, density, viscosity measurement of methionine in aqueous electrolytic solutions at 303 K. *Rasayan J. Chem.* **2010**, *3*, 550–555.
- (9) Pal, A.; Kumar, H.; Mann, R.; Sharma, H. K. Solute–solvent interactions of glycine, L-alanine, and L-valine in aqueous 1-methyl-3-octylimidazolium chloride ionic liquid solutions in the temperature interval (288.15–308.15) K. *Thermochim. Acta* **2014**, *590*, 127–137.
- (10) Nain, A. K.; Lather, M.; Sharma, R. K. Volumetric, ultrasonic and viscometric behavior of L-methionine in aqueous-glucose solutions at different temperatures. *J. Mol. Liq.* **2011**, *159*, 180–188.
- (11) Earle, M. J.; Seddon, K. R. Ionic liquids: Green solvents for the future. *Pure Appl. Chem.* **2000**, *72*, 1391–1398.
- (12) Hijo, A. A. C. T.; Maximo, G. J.; Costa, M. C.; Batista, E. A. C.; Meirelles, A. J. A. Applications of Ionic Liquids in the Food and Bioproducts Industries. *ACS Sustainable Chem. Eng.* **2016**, *4*, 5347–5369.
- (13) Kumar, H.; Sharma, R. Solvation properties of glycine and glycyglycine in aqueous 1-hexyl-3-methylimidazolium bromide solution at different temperatures. *J. Chem. Thermodyn.* **2021**, *152*, No. 106268.
- (14) Dupont, J.; F De Souza, R.; Suarez, P. A. Z. Ionic liquids (molten salt) phase organometallic catalysis. *Chem. Rev.* **2002**, *102*, 3667–3692.
- (15) Plechkova, N. V.; Seddon, K. R. Applications of ionic liquids in chemical industry. *Chem. Soc. Rev.* **2008**, *37*, 123–150.
- (16) Endres, F.; El Abedin, S. Z. Air and water stable ionic liquids in physical chemistry. *Phys. Chem. Chem. Phys.* **2006**, *8*, 2101–2116.
- (17) Wang, P.; Zakeeruddin, S. M.; Moser, J. E.; Gratzel, M.; et al. Enhance the optical absorptivity of nanocrystalline TiO₂ film with high molar extinction coefficient ruthenium sensitizers for high performance dye-sensitized solar cells. *J. Am. Chem. Soc.* **2008**, *130*, 10720–10728.
- (18) Kumar, H.; Singh, G.; Kataria, R.; Sharma, S. K. Volumetric, acoustic and infrared spectroscopic study of amino acids in aqueous solutions of pyrrolidinium based ionic liquid, 1-butyl-1-methyl pyrrolidinium bromide. *J. Mol. Liq.* **2020**, *303*, No. 112592.
- (19) Naik, K. B. K. Influence of dielectric constant on protonation equilibria of L-cysteine and L-methionine in 1, 4-dioxane-water mixture. *Global Res. Dev. J. Eng.* **2017**, *2*, 60–65.
- (20) Das, D.; Das, B.; Hazra, D. K. Conductance of some 1:1 electrolytes in N,N-dimethyl acetamide at 25 °C. *J. Solution Chem.* **2002**, *31*, 425–431.
- (21) Guha, C.; Chakraborty, J. M.; Karanjai, S.; Das, B. The structure and thermodynamics of ion association and solvation of some thiocyanates and nitrates in 2-methoxyethanol studied by conductometry and FTIR spectroscopy. *J. Phys. Chem. B* **2003**, *107*, 12814–12819.
- (22) Saini, A.; Prabhune, A.; Mishra, A. P.; Dey, R. Density, ultrasonic velocity, viscosity, refractive index and surface tension of aqueous choline chloride with electrolyte solutions. *J. Mol. Liq.* **2021**, *323*, No. 114593.
- (23) Roy, M. N.; Sikdar, P. S.; De, P. Probing Subsistence of Diverse Interplay of an Imidazolium Based Ionic Liquid Insight into Industrially Significant Solvent Environments. *Ind. J. Adv. Chem. Soc.* **2014**, *3*, 64–76.
- (24) Sinha, B.; Dakua, V. K.; Roy, M. N. Apparent molar volumes and viscosity B-coefficients of some amino acids in aqueous tetramethylammonium iodide solutions at 298.15 K. *J. Chem. Eng. Data* **2007**, *52*, 1768–1772.
- (25) Roy, M. N.; Chanda, R.; Das, R. K.; Ekka, D. Densities and viscosities of citric acid in aqueous cetrimonium bromide solutions with reference to the manifestation of solvation. *J. Chem. Eng. Data* **2011**, *56*, 3285–3290.
- (26) Chatterjee, A.; Das, B. Electrical conductances of tetrabutyl ammonium bromide, sodium tetraphenylborate, and sodium bromide in methanol (1) + water (2) mixtures at (298.15, 308.15, and 318.15) K. *J. Chem. Eng. Data* **2006**, *51*, 1352–1355.
- (27) Lind, J. E., Jr.; Zwolenik, J. J.; Fuoss, R. M. Calibration of Conductance Cells at 25° with Aqueous Solutions of Potassium Chloride. *J. Am. Chem. Soc.* **1959**, *81*, 1557–1559.
- (28) Rajbanshi, B.; Das, K.; Lepcha, K.; Das, S.; Roy, D.; Kundu, M.; Roy, M. N. Minimization of the dosage of food preservatives mixing with ionic liquids for controlling risky effect in human body: Physicochemical, antimicrobial and computational study. *J. Mol. Liq.* **2019**, *282*, 415–427.
- (29) Tiwari, A.; Honingh, C.; Ensing, B. Accurate calculation of zero point energy from molecular dynamics simulations of liquids and their mixtures. *J. Chem. Phys.* **2019**, *151*, No. 244124.
- (30) Hartnett, P. E.; Mauck, C. M.; Harris, M. A.; Young, R. M.; Wu, Y. L.; Marks, T. J.; Wasielewski, M. R. Influence of anion delocalization on electron transfer in a covalent porphyrin donor–perylene diimide dimer acceptor system. *J. Am. Chem. Soc.* **2017**, *139*, 749–756.
- (31) Lu, T.; Chen, F. Multiwfn, a multifunctional wavefunction analyser. *J. Comput. Chem.* **2012**, *33*, 580–592.
- (32) Yan, Z.; Chen, X.; Liu, C.; Cao, L. X. Molecular interactions between some amino acids and a pharmaceutically active ionic liquid domiphen DL-mandelic acid in aqueous medium at temperatures from 293.15 K to 313.15 K. *J. Chem. Thermodyn.* **2019**, *138*, 1–13.
- (33) Jamal, M. A.; Shahazidy, U.; Al-Saeed, F. A.; Al Syaad, K. M.; Muneer, M.; Ahmed, I.; Ahmed, A. E. Investigations to Explore Molecular Interactions and Sweetness Response of Polyhydroxy Compounds With Amino Acids in Aqueous Systems. *ACS Omega* **2022**, *7*, 40950–40962.
- (34) Zhao, C.; Ma, P.; Xia, S. Studies on partial molar volumes of some amino acids and their groups in aqueous solutions from 293.15 K to 333.15 K. *J. Chem. Eng. Data* **2004**, *12*, 521–526.
- (35) Yan, Z.; Wang, J.; Kong, W.; Lu, J. Effect of temperature on volumetric and viscosity properties of some α -amino acids in aqueous calcium chloride solutions. *Fluid Phase Equilib.* **2004**, *215*, 143–150.
- (36) Banerjee, T.; Kishore, N. Interactions of some amino acids with aqueous tetraethylammonium bromide at 298.15 K: a volumetric approach. *J. Solution Chem.* **2005**, *34*, 137–153.
- (37) Ghosh, B.; Sinha, A.; Roy, N.; Rajbanshi, B.; Mondal, M.; Roy, D.; Das, A.; Ghosh, N. N.; Dakua, V. K.; Roy, M. N. Molecular interactions of some bioactive molecules prevalent in aqueous ionic liquid solutions at different temperatures investigated by experimental

- and computational contrivance. *Fluid Phase Equilib.* **2022**, *557*, No. 113415.
- (38) Roy, M. N.; Dakua, V. K.; Sinha, B. Partial molar volumes, viscosity B-coefficients, and adiabatic compressibilities of sodium molybdate in aqueous 1,3-dioxolane mixtures from 303.15 to 323.15 K. *Int. J. Thermophys.* **2007**, *28*, 1275–1284.
- (39) Sharma, S. K.; Singh, G.; Kumar, H.; Kataria, R. Effect of temperature on viscometric properties of aliphatic amino acids glycine/l-alanine/l-valine in aqueous solutions of tetraethylammonium iodide. *J. Mol. Liq.* **2016**, *216*, 516–525.
- (40) Yasmin, A.; Barman, S.; Barman, B. K.; Roy, M. N. Investigation of diverse interactions of amino acids (Asp and Glu) in aqueous dopamine hydrochloride with the manifestation of the catecholamine molecule recognition tool in solution phase. *J. Mol. Liq.* **2018**, *271*, 715–729.
- (41) Banipal, P. K.; Banipal, T. S.; Ahluwalia, J. C.; Lark, B. S. Partial molar heat capacities and volumes of transfer of some saccharides from water to aqueous urea solutions at $T = 298.15$ K. *J. Chem. Thermodyn.* **2000**, *32*, 1409–1432.
- (42) Dhondge, S. S.; Deshmukh, D. W.; Paliwal, L. J.; Dahasahasra, P. N. The study of molecular interactions of ascorbic acid and sodium ascorbate with water at temperatures (278.15, 288.15 and 298.15)K. *J. Chem. Thermodyn.* **2013**, *67*, 217–226.
- (43) Jones, G.; Dole, M. The viscosity of aqueous solutions of strong electrolytes with Special reference to barium chloride. *J. Am. Chem. Soc.* **1929**, *51*, 2950–2964.
- (44) Pal, A.; Kumar, S. Viscometric and volumetric studies of some amino acids in binary aqueous solutions of urea at various temperatures. *J. Mol. Liq.* **2004**, *109*, 23–31.
- (45) Dutta, A.; Roy, K.; Basak, S.; Majumder, S.; Roy, M. N. Investigation of solution behaviour of an ionic liquid in diverse cellosolves by physicochemical contrivance. *J. Adv. Chem. Sci.* **2018**, *04*, 543–548.
- (46) Kant, S.; Kumar, A.; Kumar, S. Molar volume, viscosity and conductance studies of some alkali metal chlorides in aqueous ascorbic acid. *J. Mol. Liq.* **2009**, *150*, 39–42.
- (47) Pitkänen, I.; Suuronen, J.; Nurmi, J. Partial molar volume, ionization, viscosity and structure of Glycine betaine in aqueous solutions. *J. Solution Chem.* **2010**, *39*, 1609–1626.
- (48) Zafarani-Moattar, M. T.; Shekaari, H.; Jafari, P. Evaluation of solute–solvent interactions in aqueous solutions containing cholinium aminoate ionic liquids and polyethylene glycol dimethyl ether as a nontoxic solvent: thermodynamic and transport studies. *J. Chem. Eng. Data* **2019**, *64*, 1322–1337.
- (49) Ankita; Chand, D.; Nain, A. K. Molecular interactions of drug semicarbazide hydrochloride in aqueous-D-xylose/L-arabinose solutions at different temperatures: Volumetric, acoustic and viscometric study. *J. Chem. Thermodyn.* **2020**, *146*, No. 106106.
- (50) Zafarani-Moattar, M. T.; Shekaari, H.; Jafari, P. Volumetric, acoustic and viscometric investigation of some choline amino acid ionic liquids in aqueous solutions of polypropylene glycol 400 and polyethylene glycol 400. *J. Chem. Thermodyn.* **2020**, *142*, No. 106019.
- (51) Stokes, R. H.; Mills, R. Viscosity of electrolytes and related properties. In *The International Encyclopedia of Physical Chemistry and Chemical Physics*; Pergamon Press: Oxford, 1965.
- (52) Mondal, M.; Basak, S.; Choudhury, S.; Ghosh, N. N.; Roy, M. N. Investigation of molecular interactions insight into some biologically active amino acids and aqueous solutions of an anti-malarial drug by physicochemical and theoretical approach. *J. Mol. Liq.* **2021**, *341*, No. 116933.
- (53) Mondal, M.; Basak, S.; Rajbanshi, B.; Choudhury, S.; Ghosh, N. N.; Roy, M. N. Subsistence of diverse interactions of some biologically important molecules in aqueous ionic liquid solutions at various temperatures by experimental and theoretical investigation. *J. Mol. Struct.* **2022**, *1257*, No. 132571.
- (54) Born, M.; Wolf, E. Principles of Optics: Electromagnetic Theory of Propagation. In *Interference and Diffraction of Light*, 7th ed.; Cambridge University Press: London, 1999.
- (55) Deetlefs, M.; Seddon, K.; Shara, M. Predicting physical properties of ionic liquids. *Phys. Chem. Chem. Phys.* **2006**, *8*, 642–649.
- (56) Ekka, D.; Roy, M. N. Conductance, a contrivance to explore ion association and solvation behavior of an ionic liquid (tetrabutylphosphonium tetrafluoroborate) in acetonitrile, Tetrahydrofuran, 1,3-Dioxolane, and Their Binaries. *J. Phys. Chem. B* **2012**, *116*, 11687–11694.
- (57) Ekka, D.; Ray, T.; Roy, K.; Roy, M. N. Exploration of Solvation Consequence of Ionic Liquid [Bu₄PCH₃SO₃] in Various Solvent Systems by Conductance and FTIR Study. *J. Chem. Eng. Data* **2016**, *61*, 2187.
- (58) Majumder, S.; Sarkar, L.; Mondal, M.; Roy, D.; Roy, K.; Barman, A.; Roy, N.; Roy, M. N. Subsistence of assorted molecular interactions of substantial amino acids prevalent in aqueous solutions of ionic liquid (TBMS) probed by experimental and computational investigations. *Results Chem.* **2022**, *4*, No. 100326.
- (59) Anderson, J. L.; Pino, V.; Hagberg, E. C.; Sheares, V. V.; Armstrong, D. W. Surfactant solvation effects and micelle formation in ionic liquids. *Chem. Commun.* **2003**, *19*, 2444–2445.
- (60) Romero, C. M.; Jiménez, E.; Suárez, F. Effect of temperature on the behavior of surface properties of alcohols in aqueous solution. *J. Chem. Thermodyn.* **2009**, *41*, 513–516.
- (61) Romero, C. M.; Paéz, M. S. Surface tension of aqueous solutions of alcohol and polyols at 298.15 K. *Phys. Chem. Liq.* **2006**, *44*, 61–65.
- (62) Tan, C.-y.; Li, M.; Lin, Y.; Lu, X.; Chen, Z. Biosorption of Basic Orange from aqueous solution onto dried *A. filiculoides* biomass: Equilibrium, kinetic and FTIR studies. *Desalination* **2011**, *266*, 56–62.
- (63) Ebrahimi, F.; Sadeghizade, A.; Neysan, F.; Heydari, M. Fabrication of nanofibers using sodium alginate and poly(vinyl alcohol) for the removal of Cd²⁺ ions from aqueous solutions: adsorption mechanism, kinetics and thermodynamics. *Heliyon* **2019**, *5*, No. e02941.
- (64) Roy, D.; Majumder, S.; Rajbanshi, B.; Saha, S.; Sinha, B. Physicochemical investigation of L-Asparagine in green solvent arrangements with the manifestation of solvation consequences. *World J. Adv. Res. Rev.* **2022**, *13*, 401–428.
- (65) Zhang, J.; Zhang, S.; Dong, K.; Zhang, Y.; Shen, Y.; Lv, X. Supported Absorption of CO₂ by tetra butyl phosphonium amino acid ionic liquids. *Chem. – Eur. J.* **2006**, *12*, 4021–4026.
- (66) Scarpellini, E.; Ortolani, M.; Nucara, A.; Baldassarre, L.; Missori, M.; Fastampa, R.; Caminiti, R. Stabilization of the tensile strength of aged cellulose paper by cholinium-amino acid ionic liquid treatment. *J. Phys. Chem. C* **2016**, *120*, 24088–24097.
- (67) Zhao, H.; Jackson, L.; Song, Z.; Olubajo, O. Using ionic liquid [EMIM][CH₃COO] as an enzyme-‘friendly’ co-solvent for resolution of amino acids. *Asymmetry* **2006**, *17*, 2491–2498.
- (68) Kumar, H.; Sharma, R. Influence of 1-hexyl-3-methylimidazolium bromide ionic liquid on the volumetric and acoustic properties of amino acids (L-alanine and L-phenylalanine) at different temperatures. *J. Mol. Liq.* **2020**, *304*, No. 112666.
- (69) Dogonadze, R. R.; Kalman, E.; Kornyshev, A. A.; Ulstrup, J. *The Chemical Physics of Solvation, Part B, Spectroscopy Solvation*; Elsevier: Amsterdam, 1986.
- (70) Pople, J. A.; Schneider, W. G.; Bernstein, A. J. *High Resolution Nuclear Magnetic Resonance*; McGraw-Hill: New York, 1959.
- (71) Wiberg, K. B.; Nist, B. J.; Benjamin, W. A. *The Interpretation of NMR Spectra*; WA Benjamin: New York, 1962.
- (72) Jackman, L. M. *Nuclear Magnetic Resonance Spectroscopy*, Pergamon: New York, 1959.
- (73) Ebersson, L.; Farsen, S. Proton magnetic resonance studies on intramolecular hydrogen bonding in mono-anions of sterically hindered succinic acids. *J. Phys. Chem. A* **1960**, *64*, 767–769.
- (74) Andrew, E. R.; Bradbury, A.; Eades, R. G.; Jenks, G. F. Fine Structure of the Nuclear Magnetic Resonance Spectra of Solids: Chemical Shift Structure of the Spectrum of Phosphorus Pentachloride. *Nature* **1960**, *188*, 1096–1097.
- (75) Chen, H.-Y.; Fang, S.; Wang, L. Interactions of 1-butyl-2,3-dimethylimidazolium bromide ionic liquid with glycine, L-alanine and

L-valine: A volumetric and NMR spectroscopic study. *J. Mol. Liq.* **2017**, *225*, 706–712.

(76) Bonhôte, P.; Dias, A. P.; Papageorgiou, N.; Kalyanasundaram, K.; M Grätzel, M. Hydrophobic, highly conductive ambient-temperature molten salts. *Inorg. Chem.* **1996**, *35*, 1168–1178.

(77) Caso, J. V.; Russo, L.; Palmieri, M.; Malgieri, G.; Galdiero, S.; A Falanga, A.; Isernia, C.; Iacovino, R. Investigating the inclusion properties of aromatic amino acids complexing beta-cyclodextrins in model peptides. *Amino Acids* **2015**, *47*, 2215–2227.

(78) Kumar, S.; Sagar, S.; Gupta, M. A thermodynamic and ¹H NMR spectroscopy study of binary mixtures of polyethylene glycol butyl ether (PEGBE) 206 with 1-Butanol and 2-(Methylamino) ethanol (MAE). *J. Mol. Liq.* **2016**, *214*, 306–312.

(79) Rajbanshi, B.; Saha, S.; Das, K.; Barman, B. K.; Sengupta, S.; Bhattacharjee, A.; M N Roy, M. N. Study to probe subsistence of host-guest inclusion complexes of α and β -cyclodextrins with biologically potent drugs for safety regulatory discharge. *Sci. Rep.* **2018**, *8*, No. 13031.

(80) Roy, M. N.; Saha, S.; Barman, S.; Ekka, D. Host-guest inclusion complexes of RNA nucleosides inside aqueous cyclodextrins explored by physicochemical and spectroscopic methods. *RSC Adv.* **2016**, *6*, 8881–8891.

(81) Slavchov, R. I.; Novev, J. K. Surface tension of concentrated electrolyte solutions. *J. Colloid Interface Sci.* **2012**, *387*, 234–243.

(82) Contreras-García, J.; Johnson, E. R.; Keinan, S.; Chaudret, R.; Piquemal, J.-P.; Beratan, D. N.; Yang, W. NCIPLLOT: a program for plotting noncovalent interaction regions. *J. Chem. Theory Comput.* **2011**, *7*, 625–632.